Antagonist actions of CMK-1/CaMKI and TAX-6/Calcineurin along the *C. elegans* thermal avoidance circuit orchestrate adaptation of nociceptive response to repeated stimuli

Martina Rudgalvyte[1], Zehan Hu[1], Dieter Kressler[1,2], Joern Dengjel[1], and Dominique A. Glauser[1,3]

[1], Department of Biology, University of Fribourg, 1700 Fribourg, Switzerland

[2], Metabolomics and Proteomics Platform (MAPP), Department of Biology, University of Fribourg, 1700 Fribourg, Switzerland

[3], Corresponding author dominique.glauser@unifr.ch

ABSTRACT

Response decrease following repeated exposure to innocuous or noxious stimuli is a conserved adaptation phenomenon often referred to as habituation. Impaired nociceptive habituation is associated with several pain conditions in human, but the underpinning molecular mechanisms are only partially understood. In the nematode *Caenorhabditis elegans*, thermo-nociceptive adaptation to repeated stimuli was previously shown to be regulated by the Ca^{2+}/Calmodulin-dependent protein kinase 1 (named CMK-1), but its downstream effectors were unknown. Here, using *in vitro* kinase assays coupled with mass-spectrometry-based phosphoproteomics, we empirically identified hundreds of CMK-1 phospho-substrates. Among them, we found that CMK-1 can phosphorylate the calcineurin A (CnA) protein TAX-6 *in vitro* in a highly conserved regulatory domain, which led us to hypothesize that TAX-6/CnA might be a downstream mediator of CMK-1 signaling in the control of thermo-nociceptive adaptation. Combined genetic and pharmacological manipulations revealed a network of antagonistic actions between CMK-1 and calcineurin pathways in the regulation of the responsiveness of naïve worms and the response adaptation to repeated noxious heat stimuli. However, the results of cell-specific rescue and gain-of-function experiments suggested that CMK-1 acts in AFD and ASER thermosensory neurons and that TAX-6/CnA acts in FLP thermosensory neuron and a set of downstream interneurons to regulate noxious heat avoidance behaviors. Because CMK-1 and TAX-6/CnA act in non-overlapping cell types, the phosphorylation event identified *in vitro* might not be relevant for this phenotype and the complex interaction between the two pathways might rather originate from their action in separate parts of the nervous system. As a whole, our study has identified (i) CMK-1 substrate candidates, which will fuel further research on the intracellular actuation of CMK-1-dependent signaling on various processes, and (ii) a complex set of antagonistic interactions between CMK-1 and calcineurin signaling operating at distributed loci within a sensory-behavior circuit, acting to adjust baseline thermo-nociception and regulate thermo-nociceptive adaptation.

INTRODUCTION

Animals from invertebrates to mammals can detect and avoid harmful stimuli, which is essential for their survival and well-being. Noxious stimuli are detected and encoded by specialized primary sensory neurons in a process called nociception (Dubin and Patapoutian 2010). Nociceptive signals are relayed in the nervous system via synaptic connections to be further processed and trigger different responses, such as behavioral changes and the perception of pain (Treede 1995). Pain sensitivity is not fixed and can be adjusted in various physiological and pathological contexts through nociceptive plasticity processes such as hyperalgesia or nociceptive desensitization/habituation (Kidd and Urban 2001, Sandkühler 2009, Rodriguez-Raecke, Doganci et al. 2010, Breimhorst, Hondrich et al. 2012, May, Rodriguez-Raecke et al. 2012, O'Neill, Brock et al. 2012, Basith, Cui et al. 2016). Prolonged or repeated exposure to noxious stimuli can lead to either sensitization or desensitization/habituation depending on the stimuli intensity, frequency and various physiological factors (Treede 1995). Because impaired nociceptive habituation is linked to various human chronic pain conditions (de Tommaso, Lo Sito et al. 2005, Smith, Tooley et al. 2008, de Tommaso, Federici et al. 2011), obtaining a deeper understanding of the cellular and molecular processes into play appears highly relevant to aid in the development of new therapeutical strategies for pain management. Several molecular mechanisms have been shown to modulate nociceptive pathways from the periphery to the brain (Kuner and Flor 2017, Pace, Passavanti et al. 2018, Amna, Salman et al. 2019), which involve the regulated activity of proteins such as membrane receptors or ion channels (involved in sensory-transduction, cell excitability, or signal conduction). Many kinases and phosphatases, which actuate protein regulation via the control of their phosphorylation status and that were previously shown to broadly regulate neural plasticity in the nervous system, are also involved in nociceptive plasticity (Willis Jr. 2001, Fu, Han et al. 2008, Wang and Zhang 2012, Isensee, Diskar et al. 2014, Pace, Passavanti et al. 2018). These regulatory pathways include intracellular signaling by calcium/calmodulin-dependent protein kinases (CaMKs) (Shum, Ko et al. 2005, Liang, Liu et al. 2012, Schild, Zbinden et al. 2014, Zhou, Liu et al. 2017), which might couple cellular activity levels with pleiotropic intracellular effects via post-translational modifications over a large repertoire of potential target proteins. Identifying the phosphorylation substrates of these kinases that act in the nociceptive pathway to mediate plasticity effects could provide relevant insight for future pain management translational research.

The nematode *Caenorhabditis elegans* has emerged as a powerful model to study the molecular and cellular bases of nociception and its plasticity. *C. elegans* produces innate avoidance behaviors in response to a variety of noxious stimuli, including irritant chemicals, harsh touch and noxious heat (Kaplan and Horvitz 1993, Wittenburg and Baumeister 1999, Hilliard, Apicella et al. 2005, Li, Kang et al. 2011, Liu, Schulze et al. 2012). Noxious heat stimuli targeting the animal head or the entire animal trigger a stereotyped reversal behavior (Wittenburg and Baumeister 1999, Liu, Schulze et al. 2012, Byrne Rodgers and Ryu 2020, Lia and Glauser 2020), which involves several thermo-sensory neurons, including AFD, AWC, and FLP, proposed to work as thermo-nociceptors (Chatzigeorgiou and Schafer 2011, Liu, Schulze et al. 2012, Kotera, Tran et al. 2016). The molecular components underpinning the function of the nociceptive system are well-conserved.

E.g., transient receptor potential (TRP) channels mediate worm thermo-nociceptive responses, like in fly and mammals (Chatzigeorgiou, Yoo et al. 2010, Glauser, Chen et al. 2011, Liu, Schulze et al. 2012, Nkambeu, Salem et al. 2020). Furthermore, persistent or repeated noxious heat stimuli cause a progressive reduction in the rate of heat-evoked reversals (Lia and Glauser 2020, Jordan and Glauser 2023), which we will refer to here as thermo-nociceptive adaptation. A genetic screen for human pain-associated gene orthologs revealed thermo-nociceptive adaptation alterations for many corresponding worm mutants, substantiating the interest of the model (Jordan and Glauser 2023). Among conserved molecular players, the worm CaMKI (named CMK-1) was shown to mediate thermo-nociceptive adaptation (Schild, Zbinden et al. 2014, Lia and Glauser 2020, Jordan and Glauser 2023). CMK-1 is broadly expressed in the worm nervous system and, beyond thermo-nociceptive adaptation, controls multiple experience-dependent plasticity processes, such as those related to developmental trajectories (Neal, Takeishi et al. 2015), the encoding of preferred growth temperature (Yu, Bell et al. 2014), salt aversive learning (Lim, Fehlauer et al. 2018) and habituation to repeated touch stimuli (Ardiel, McDiarmid et al. 2018). CMK-1 was shown to regulate the expression of the *guanylyl cyclase-8* (*gcy-8*) gene (Satterlee, Ryu et al. 2004), the AMPA glutamate receptor-1 (*glr-1)* gene (Moss, Park et al. 2016), the ortholog of the human DACH1/2 Dachsund transcription factor gene *(dac-1)* and the PY domain transmembrane protein-1 (*pyt-1*) gene (Harris, Bates et al. 2023). The impact of CMK-1 on gene transcription is partially mediated by the CREB homolog-1 (CRH-1) transcription factor (Harris, Bates et al. 2023), which could be phosphorylated by CMK-1 *in vitro* (Kimura, Corcoran et al. 2002) and in an heterologous expression system (Eto, Takahashi et al. 1999). A previous study used an *in silico* approach to systematically predict potential CMK-1 phosphorylation substrates and revealed repeated-touch habituation phenotypes in mutants for several candidate targets (Ardiel, McDiarmid et al. 2018). Apart from these few studies, we still know very little on the CMK-1 downstream effectors that mediate the numerous biological actions of CMK-1, including in mediating thermo-nociceptive adaptation.

Calcineurin is a well-conserved eukaryotic Ca^{2+}/Calmodulin activated Serine/Threonine phosphatase (Klee, Crouch et al. 1979, Rusnak and Mertz 2000), involved in Ca^{2+} signaling pathway and functioning in several tissues, such as muscles, T cells and neurons, where it regulates synaptic plasticity and memory (Groth, Dunbar et al. 2003, Mukherjee and Soto 2011). Calcineurin regulates the activity of numerous proteins, such as transcription factors (Molkentin 2004), receptors, mitochondria proteins and microtubules depending on Ca^{2+} signaling state (Peuker, Strigli et al. 2022). Overexpression of calcineurin can cause cardiac hypertrophy (Gillis, Kavanagh et al. 2004, Yuan, Shen et al. 2024), higher infarct volumes (Dai, Hu et al. 2024), whereas lack of function can cause defects in kidney development (Gooch, Toro et al. 2004), and increase in autophagy (Ke, Huang et al. 2023). Chronic inhibition of calcineurin with immunosuppressant drugs, like cyclosporin A, was shown to cause irreversible neuropathic pain in some patients, a phenomenon referred to as calcineurin inhibitor-induced pain syndrome (Smith 2009). Several studies in mice have highlighted that calcineurin signaling modulate thermal nociception (Sato, Onaka et al. 2007). Several pathways working downstream of calcineurin signaling have been proposed to mediate the regulation of nociception, including NFAT transcription factors, TWIK-related spinal cord potassium channels (TRESK), TRP channels, and α2δ-1 Ca^{2+} channels (Smith

122 2009, Huang, Chen et al. 2020, Huang, Chen et al. 2022). Nevertheless, we still have a cursory
123 understanding of how calcineurin signaling integrates with other intracellular signaling pathways
124 at different locus in the nociceptive circuit to orchestrate nociceptive plasticity.

125 Calcineurin is a heterodimeric protein consisting of one calcineurin A (CnA) catalytic subunit, and
126 one calcineurin B (CnB) regulatory subunit. CnA contains catalytic and autoinhibitory domains,
127 as well as CnB and Ca^{2+}/Calmodulin binding domains. In the absence of Ca^{2+} signaling, the
128 autoinhibitory domain suppresses catalytic phosphatase activity. Increase in cytosolic Ca^{2+}
129 promotes Ca^{2+} binding to CnB and to CaM. Ca^{2+}/CnB and Ca^{2+}/CaM in turn bind to calcineurin A
130 subunit to release the autoinhibition, allow substrates to access the active site and thereby the
131 activation of CnA (Bandyopadhyay, Lee et al. 2002, Kuhara, Inada et al. 2002, Wang, Du et al.
132 2008). *Caenorhabditis elegans* genome encodes one CnA homolog *tax-6 (*aka *cna-1)*, and one
133 CnB homolog *cnb-1* displaying conserved structural and biochemical features with vertebrate
134 calcineurin proteins (Bandyopadhyay, Lee et al. 2002, Bandyopadhyay, Lee et al. 2004). Lack of
135 *tax-6* function causes thermal hypersensitivity and increased osmosensation, as well as
136 increased adaptation of olfactory system (Kuhara, Inada et al. 2002). Loss-of-function mutants
137 display a thermophilic behavior, and this anomaly could be rescued by wild type *tax-6* expression
138 in AFD neurons. *tax-6* gain-of-function mutants show defective enteric muscle contraction (Lee,
139 Song et al. 2005), as well as higher brood size and hypersensitivity to serotonin (Lee, Jee et al.
140 2004). The loss of *cnb-1* causes lethargic movements, delayed egg laying and reduced growth
141 (Bandyopadhyay, Lee et al. 2002).

142 Here, we combined *in vitro* kinase assays with shotgun phosphoproteomics to empirically identify
143 CMK-1 phospho-substrates in worm peptide and protein libraries. CMK-1 was found to
144 phosphorylate TAX-6/CnA in a highly conserved regulatory region, suggesting cross-regulation
145 between CaMK and calcineurin signaling in worms. We next combined genetic and
146 pharmacological manipulations with a quantification of noxious heat reversals to assess the role
147 of CMK-1 and TAX-6 signaling and their interactions in controlling naïve animal responsiveness
148 and the adaptation to repeated stimulation. These follow-up analyses confirmed a complex set of
149 antagonistic signaling actions produced by the two pathways. However, the two intracellular
150 signaling pathways appear to primarily function in separate neuron types to control thermo-
151 nociceptive adaptation indicating that the phosphorylation of TAX-6/CnA by CMK-1 might not be
152 relevant *in vivo* for the control of thermo-nociception. Collectively, our results reveal multiple
153 direct and indirect interactions between CaMK and calcineurin signaling and pave the role for
154 deeper studies on the molecular control of nociceptive adaptation in a simple genetic model.

155

156

157 **RESULTS**

158

159 **CMK-1 phosphorylates multiple substrates *in vitro* including TAX-6/CnA**

160 To identify phosphorylation substrates of CMK-1, we performed *in vitro* kinase assays on two
161 types of substrate libraries followed by mass spectrometry-based phosphoproteomics (Fig. 1A).
162 To that end, we purified recombinant CMK-1(1-295)T179D mutant protein produced in *E. coli*.
163 This mutant is a constitutively active form of CMK-1 that lacks the C-terminal auto-inhibitory
164 domain and harbors a T179D phosphomimic mutation, thus bypassing the need for Ca^{2+}/CaM
165 binding and for phosphorylation by CKK-1. In two separate experiments, we assessed the
166 phosphorylation produced by CMK-1(1-295)T179D, first, on a library of worm peptides produced
167 by trypsin digestion of whole protein extracts and, second, on a whole protein library produced
168 in non-denaturing conditions. As expected given the strong structural and functional
169 conservation within the CaM kinase family, the consensus substrate motifs obtained with each
170 substrate libraries matched the ΦXRXX(S/T)XXXΦ consensus previously characterized for
171 mammalian CaMK (where Φ represents hydrophobic residues, Fig. 1B) (Lee, Kwon et al. 1994,
172 White, Kwon et al. 1998). This result supports the validity of our *in vitro* kinase assays to identify
173 direct CMK-1 targets and indicates that our experimental design efficiently mitigated the impact
174 of any potential kinase activity coming from *E. coli* protein contamination or from worm kinases
175 in the case of whole protein extracts.

176 With the peptide library data, we identified 646 phosphosites in 478 proteins (File S1). With the
177 whole protein library, we identified 427 phosphosites in 365 proteins (File S1). Fifty-one
178 phosphosites in 50 proteins were common between the two datasets (File S1, Fig.1B). As more
179 extensively discussed later in the text (see Discussion section), these datasets are expected to
180 include both phosphosites that are relevant CMK-1 target *in vivo* and 'false positive'
181 phosphosites which are not relevant targets *in vivo*. These datasets are also expected to be
182 biased toward abundant proteins, which are more likely to be detected. Consistent with this
183 expectation, the most significant enrichment found via gene ontology (GO) term analyses in
184 related to ribosomal and cytoskeletal proteins (File S2). Outside of these categories and among
185 the phosphosites common to our two datasets, we were intrigued by the presence of a CMK-1
186 target phosphosite on the serine 443 of TAX-6/CnA. This phosphosite is located in a highly
187 conserved region of TAX-6/CnA regulatory domain, just on the C-terminal side of the CaM
188 binding domain (Fig. 1D). To confirm that CMK-1 can phosphorylate TAX-6/CnA S443 *in vitro*, we
189 repeated the kinase assay using recombinant TAX-6/CnA protein purified from *E. coli* as
190 substrate. Abundant phosphorylation of S443 was observed upon treatment with the
191 constitutively active CMK-1 form, whereas this phosphorylation remained undetected with
192 kinase-dead control treatment (Fig. 1C). We conclude that CMK-1 can phosphorylate TAX-6/CnA
193 on S443 *in vitro*.

194

195 **Thermo-nociceptive adaptation is impaired by CMK-1 down-regulation and by both up- and**
196 **down-regulation of TAX-6/CnA**

197 We previously reported that CMK-1 controls the adaptation to persistent noxious heat
198 stimulations (Schild, Zbinden et al. 2014) or repeated stimulations (Lia and Glauser 2020). This
199 adaptation effect consists in a progressive reduction of the noxious heat-evoked reversal
200 response observed in wild type during one hour of repeated heat stimulation. Importantly, this
201 adaptation effect does not result from thermal damages or from an exhaustion of neuronal or
202 muscular tissues, as evidenced by the existence of non-adapting mutants which can maintain a
203 constant response level (Jordan and Glauser 2023). We confirmed these previous observations
204 by quantifying heat-evoked reversals in naïve animals (T0) and animals submitted to a series of
205 repeated heat stimulation for one hour (T60, *adaptation treatment* with an interstimulus interval
206 (ISI) of 20 s, Fig. 2A). Whereas wild type response is significantly decreased following repeated
207 stimulation treatment (1h adaptation, T60), this adaptation effect is absent in a *cmk-1(ok287)*
208 loss-of-function mutants (Fig. 2B). Conversely, a *cmk-1(syb1633)* gain-of-function mutant with a
209 CMK-1(T179D) over-activating mutation promoted a faster adaptation (Fig. 2B and Fig. 2-
210 supplement 1). Therefore, our data confirm that CMK-1 activity is necessary and sufficient to
211 promote thermo-nociceptive adaptation.

212 Since TAX-6/CnA is a CMK-1 kinase substrate *in vitro*, we hypothesized that it could take part in
213 the regulation of thermo-nociceptive adaptation and evaluated the impact of genetic and
214 pharmacological manipulations down-regulating or up-regulating calcineurin signaling activity.
215 The permanent loss of TAX-6/CnA in *tax-6(p675)* mutants or of CnB/CNB-1 in a *cnb-1(jh103)* and
216 *cnb-1(ok276)* mutants caused a marked elevation in the rate of spontaneous reversals (Fig. 2-
217 supplement 2). While this observation indicates that TAX-6/CnA signaling regulates reversal
218 behavior, the elevation was so high that it precluded quantifying heat-evoked reversals and
219 plasticity response. We next turned to a pharmacological approach using the calcineurin
220 inhibitor Cyclosporin A (Liu, Farmer et al. 1991). Treating wild type worms with 10 mM
221 Cyclosporin A for 24 h prior to behavioral assays did not cause the problematic elevated
222 spontaneous reversal phenotype, but significantly reduced the thermal adaptation effect
223 (Fig.2C). An intact calcineurin signaling is therefore required for thermo-nociceptive adaptation.
224 Next, we examined the impact of over-activating TAX-6/CnA, using a *tax-6(jh107)* gain-of-
225 function mutant lacking the auto-inhibitory C-terminal domain of TAX-6/CnA, which we will refer
226 to as *tax-6(gf)*. We noted a very slightly enhanced reversal response in naïve *tax-6(gf)* mutants in
227 comparison to wild type (Fig. 2D). More strikingly, the adaptation effect in *tax-6(gf)* mutants was
228 strongly impaired. Therefore, our data show that both overactivation and inhibition of TAX-6/CnA
229 signaling can block thermo-nociceptive adaptation.

230 In summary, gain- and loss-of-function analyses highlight a CMK-1-dependent pathway
231 promoting and potentially two antagonistic TAX-6/CnA-dependent pathways that promote and
232 inhibit thermo-nociceptive adaptation, respectively.

233

234 **CMK-1 and TAX-6/CnA signaling regulates thermo-nociceptive adaptation through a set of**
235 **inhibitory cross-talks**

236 To assess the potential interactions between CMK-1 and calcineurin signaling in the control of
237 thermo-nociceptive adaptation, we systematically tested combinations of up- or down-
238 regulating manipulations in the two pathways.

239 First, we examined the impact of down-regulating both CMK-1 and TAX-6/CnA signaling by
240 treating *cmk-1(lf)* mutants with Cyclosporin A. Surprisingly, whereas separate down-regulation
241 of either CMK-1 or TAX-6/CnA pathway strongly blocked adaptation, their joint down-regulation
242 caused animals to adapt like wild type (Fig. 3A). An intact adaptation when both pathways are
243 inhibited supports the notion that CMK-1 and TAX-6/CnA represent regulators of one or more
244 adaptation pathways that can also operate independently. In addition, this observation supports
245 a model in which (i) the anti-adaptation effect caused by CMK-1 inhibition is mediated by TAX-
246 6/CnA and, conversely, (ii) that the anti-adaptation effect caused by TAX-6/CnA inhibition
247 requires intact CMK-1 activity.

248 Second, we tested the impact of simultaneously activating CMK-1 and calcineurin pathways by
249 examining the behavior of *cmk-1(gf);tax-6(gf)* double mutants. We found that the double
250 mutants behaved like *tax-6(gf)* single, entirely lacking adaptation (Fig. 3B). Therefore, the pro-
251 adaptation effect of the CMK-1(T179D) activating mutation is fully blocked by TAX-6/CnA
252 overactivation, which is compatible with a model in which CMK-1 over-activation might work by
253 inhibiting calcineurin signaling.

254 Third, we assessed the impact of concomitantly up-regulating calcineurin and down-regulating
255 CMK-1 signaling, by examining the behavior of *cmk-1(lf);tax-6(gf)* double mutants. Whereas the
256 main phenotypic feature in each single mutant was a lack of adaptation, the mutation
257 combination produced a synthetic effect massively elevating spontaneous reversal, which
258 precluded quantifying heat-evoked reversals (Fig. 2-supplement 2).

259 Fourth, we tested the effect of concomitantly up-regulating CMK-1 activity and inhibiting
260 calcineurin signaling by treating *cmk-1(gf)* mutants with Cyclosporin A. We found that, unlike in
261 *cmk-1(wt)* background, Cyclosporin A treatment in *cmk-1(gf)* mutants did not prevent thermo-
262 nociceptive adaptation (Fig.3C). The fact that an overactive CMK-1 signaling can compensate for
263 the inhibition of TAX-6/CnA suggests that the anti-adaptation effect of calcineurin inhibition
264 involves the ability to down-regulate CMK-1 signaling. Furthermore, the ability of CMK-1
265 overactivation to promote adaptation when calcineurin is inhibited indicate that at least one
266 CMK-1 regulatory branch works independently or downstream of calcineurin signaling.

267 Collectively, our results do not support a simple linear model in which CMK-1 would only work
268 upstream of TAX-6/CnA. Instead, our data suggest a model in which thermo-nociceptive
269 adaptation processed are regulated via the antagonist actions of CMK-1 and TAX-6/CnA signaling
270 operating through a non-linear inhibitory network, such as the one depicted in Figure 3D and
271 discussed below (see Discussion section).

272

273 **CMK-1 acts in AFD and ASER sensory neurons to promote thermo-nociceptive adaptation**

274 Our next goal was to assess the place of action of CMK-1 signaling in the promotion of thermo-
275 nociceptive adaptation. To that end we used a neuron-specific rescue approach in the *cmk-1(lf)*
276 background. We started our experiments by restoring CMK-1 expression in candidate thermo-
277 sensory neurons, using *mec-3p* promoter to drive expression in FLP and *tax-4p* promoter to drive
278 expression in AFD, AWC, ASI and ASE, as well as *glr-1p* promoter to drive expression in a subset
279 of interneurons known to mediate reversal response. A positive control using *cmk-1p* promoter
280 showed a partial, yet significant rescue effect (Fig. 4A). We observed a strong rescue effect with
281 the *tax-4p* promoter, but no rescue effect with *mec-3p* or *glr-1p* (Fig. 4A). While not ruling out a
282 contribution of other neurons, these data point to *tax-4*-expressing neurons as a major place of
283 action for CMK-1 in the control of thermo-nociceptive adaptation.

284 To further dissect the contribution of *tax-4*-expressing neurons, we conducted additional rescue
285 experiments using *gpa-4p* to target ASI, a combination of *str-2p* and *srsx-3p* to target the two
286 AWC neurons (AWCon and AWCoff, respectively), a combination of *gcy-5p* and *gcy-6p* to target
287 ASEL and ASER neurons, *gcy-6* alone to target ASEL, *gcy-5p* alone to target ASER and *ttx-1p* to
288 target AFD. We observed an almost total rescue effect with the *ttx-1p* promoter (AFD) and a more
289 partial rescue effect with either *gcy-5p+gcy-6p* (both ASEL and ASER) or *gcy-5p* alone (only
290 ASER) (Fig. 4B). No rescue effect was observed with the other promoters. We additionally tested
291 the combined use of *ttx-1p* and *gcy-5p* to target both AFD and ASER and obtained a maximal
292 rescue effect even stronger than with *ttx-1p* alone (Fig. 4B). Taken together, out data point to AFD
293 as a major (and to ASER as a more minor) place of action for CMK-1 signaling in the control of
294 thermo-nociceptive adaptation to repeated heat-stimuli.

295 To further asses the role of AFD neurons, we evaluated the behavior of animals with genetically
296 ablated AFD neurons. Interestingly, AFD neurons were dispensable for heat-evoked reversal
297 responses in naïve animals under our experimental conditions, but required for the thermo-
298 nociceptive adaptation (Fig. 4.C). We observed similar results when selectively inhibiting AFD
299 neurotransmission in animals expressing the tetanus toxin (TeTx) in AFD (Fig. 4C).

300 Taken together, our results show that AFD neurons mediate thermo-nociceptive adaptation and
301 that intact CMK-1 signaling and neurotransmission in these neurons is essential for this process
302 (Fig. 4D). ASER might represent an additional locus of CMK-1 action with a milder quantitative
303 contribution to the process (Fig. 4D).

304

305 **TAX-6/CnA activity in RIM and command interneurons inhibits thermo-nociceptive**
306 **adaptation**

307 In order to assess the cellular place of action of TAX-6/CnA in the control of thermo-nociceptive
308 adaptation, we used a neuron-type-specific overactivation approach. We created transgenes
309 containing a *tax-6(gf)* cDNA to drive the expression of the overactive, truncated form of TAX-
310 6/CnA encoded in the *tax-6(jh107)* mutant. Like for CMK-1 rescue experiments above, we started
311 by targeting candidate thermosensory neurons using either the *mec-3p* (FLP) or *tax-4p* (AFD,
312 AWC, ASI and ASE) promoters, as well as interneurons with the *glr-1p* promoter. We examined

the ability of the transgenes to replicate the two noticeable phenotypes of *tax-6(gf)* mutants: a slightly enhanced response in naïve animals and a strong impairment of adaptation.

First, regarding naïve animal response, we found that *[mec-3p::tax-6(gf)]* and, to a lesser extent *[glr-1p::tax-6(gf)],* transgene caused a slight elevation in the heat-evoked response, whereas *[tax-4p:tax-6(gf)]* did not produce any effect (Fig. 5A). *glr-1p* promoter drives expression in several interneurons, including AVA, AVD, AVE and RIM whose activity is required and sufficient to trigger reversals (Alkema, Hunter-Ensor et al. 2005, Gray, Hill et al. 2005, Guo, Hart et al. 2009). To further dissect the specific interneurons involved, we expressed the *tax-6(gf)* transgene in AVA, AVD and AVE using the *nmr-1p* promoter, or the *lgc-39p* promoter, in RIM (and RIC) using the *cex-1p* promoter, and only in RIM using the *tdc-1p* promoter (Brockie, Mellem et al. 2001, Lemieux, Cunningham et al. 2015, Thapliyal, Beets et al. 2023). With all four promoters, we observed an effect similar to that with *glr-1p*. Taken together, these results indicate that over-activating calcineurin signaling in *mec-3p*-expressing neuron (most likely in FLP thermo-nociceptor) or in a subset of reversal-mediating interneurons such as RIM or AVA/AVD/AVE is sufficient to up-regulate noxious heat-responsiveness in naïve animals (Fig. 5C, top).

Second, regarding adaptation to repeated heat stimuli, we found that the *[glr-1p::tax-6(gf)]* transgene could significantly reduce the adaptation effect, leaving stronger response as compared to wild type after one hour of repeated stimulation (Fig. 5A). This effect was not as strong as the effect in *tax-6(gf)* mutant, which could be due to the transgene overexpression, mosaicism in the transgenic animals or to the fact that TAX-6/CnA overactivation in additional (unidentified) neurons could be also needed to reach the full effect. In contrast, the *[mec-3p::tax-6(gf)]* transgene did not affect nociceptive adaptation, whereas the *[tax-4p::tax-6(gf)]* transgene produced a slight enhancement of adaptation ($p<.05$). The data in Fig. 5A suggest that one or more *glr-1*-expressing interneurons represent a major place of action in which overactive TAX-6/CnA signaling can act to inhibit adaptation. We deepened the circuit analysis with additional promoters and observed a marked adaptation defect caused with *cex-1p* and *tdc-1p* promoters, similar to that with *glr-1p* promoter, and a milder defect with *lgc-39p* and *nmr-1p* promoter. These results point to RIM second layer interneurons as primary locus and AVA/AVD/AVE reversal command neurons as secondary locus of overactive TAX-6/CnA action, while not ruling out the implication of additional neurons (Fig. 5C bottom).

346 **DISCUSSION**

347 **CMK-1 substrate specificity is indistinguishable from that of mammalian CaMKs**

348 Our knowledge on CaMK substrate specificity comes from numerous previous biochemical
349 studies on mammalian CaMKs using synthetic peptide substrates at different scales (Lee, Kwon
350 et al. 1994, White, Kwon et al. 1998, Corcoran, Joseph et al. 2003, Johnson, Yaron et al. 2023).
351 Our study complements and extends this previous work through a large-scale identification of
352 CaMKI substrates with endogenous peptide and protein libraries. With a dataset comprising
353 several hundred substrates, we could confirm the ΦXRXX(S/T)XXXΦ consensus (where Φ
354 represents hydrophobic residues) (Lee, Kwon et al. 1994, White, Kwon et al. 1998). These
355 findings suggest that (i) the vast majority of our hits are direct CMK-1 substrates *in vitro* and (ii)
356 the substrate specificity is conserved from worm to mammals.

357 **Large-scale empirical identification of CMK-1 phospho-targets**

358 We have identified several hundred substrates that can be directly phosphorylated by CMK-1 *in*
359 *vitro*. Our hit list is expected to include both substrates that are relevant *in vivo* and substrates
360 that are not. Indeed, both the peptide library and the whole protein library datasets could
361 include phosphosites coming from proteins that never encounter CMK-1 *in vivo*: e.g., non-
362 neuronal proteins, secreted proteins, or proteins residing in specific organelles. Furthermore,
363 both datasets are expected to be biased toward abundant proteins, which are more likely to be
364 detected. Accordingly, the strongest GO term enrichments in both datasets related to abundant
365 and ubiquitous cellular components, involved in the translation process and cytoskeleton. Even
366 if we cannot rule out an actual inclination of the CaM kinase pathway to regulate these
367 processes, we suspect that these GO term enrichments rather reflect an analytical bias toward
368 abundant proteins.

369 The relatively low overlap between the peptide and the protein library datasets can be explained
370 by multiple effects. First, the peptide library dataset is expected to include phosphosites in
371 protein regions that are usually inaccessible to CMK-1 because of protein folding or protein
372 complex formation (increasing the false positive rate in the peptide library). Second, the trypsin-
373 bases cleavage prior to CMK-1 exposure in the peptide library protocol might impair proper
374 substrate recognition by the kinase (increasing false negative rate in the peptide library). Third,
375 we have chosen quite strict criteria and applied them separately to define each hit list. For
376 theoretical reasons, because substrates were presented to the kinase in a more native
377 condition, we tend to give more trust the protein library dataset, with the subset of targets also
378 found in the peptide library as top hits.

379 A previous study reported a list of 533 CMK-1 candidate substrates based on *in silico* predictions
380 (Ardiel, McDiarmid et al. 2018). We found very little overlap between those predictions and our
381 empirical datasets, with only 5 phosphosites shared with our peptide library list and 1 with our
382 protein library list (Fig. 1-supplement 1). This limited overlap could be explained either by a
383 limited exhaustiveness across the three datasets (high false negative rate) or come from
384 limitations affecting *in silico* predictions. In support of the second explanation, we note that the
385 previously predicted phosphosite list only very partially matches the empirically determined

386 CMK-1 substrate consensus (Fig. 1-supplement 1). Because we lack a solid reference point, it is
387 nevertheless hard to estimate the false positive and false negative rates in our analyses at this
388 stage. Additional experiments will be required to determine if the phosphorylation of these
389 substrates is relevant *in vivo*, potentially on a case-by-case basis. Eventually, and keeping these
390 limitations in mind, we believe that our large-scale dataset on the substrates which can by
391 phosphorylated by CMK-1 *in vitro* will represent a useful resource in the search for CMK-1/CaMKI
392 substrates mediating its numerous biological functions *in vivo*.

393 **The phosphorylation of TAX-6/CnA by CMK-1/CaMKI**

394 Previous *in vitro* studies have found that CnA can be phosphorylated by protein kinase C, casein
395 kinase I, casein kinase II, protein kinase C and by CaM kinase II (Hashimoto, King et al. 1988,
396 Hashimoto and Soderling 1989, Calalb, Kincaid et al. 1990, Rusnak and Mertz 2000). We are not
397 aware of any study having shown that CnA is a substrate of CaM kinase I. Here, we show that *C.*
398 *elegans* CaMKI CMK-1 can phosphorylate TAX-6/CnA on S443. This specific phosphorylation
399 event was confirmed in three different types of kinase assays: one using a peptide library, one
400 using a protein library, and one using purified recombinant TAX-6/CnA as substrate. Ser 443 is
401 located just downstream of the CaM binding domain in a highly conserved region (Fig. 1D and E).
402 This conserved serine was previously identified as a target of mammalian CaMKII *in vitro*
403 (Hashimoto, King et al. 1988, Hashimoto and Soderling 1989). Because TAX-6/CnA and CMK-1
404 seem to mostly work from distinct neuronal cell-type to control nociceptive adaptation, it
405 remains unclear whether TAX-6/CnA phosphorylation by CMK-1 is directly relevant for the
406 control of this process *in vivo*. Nevertheless, since the expression patterns of CMK-1 and TAX-
407 6/CnA largely overlap and since they are both activated by calcium signaling, we speculate that
408 this phosphorylation event might be relevant to other neuronal regulatory signaling and we
409 suggest it should be considered in future studies addressing the potential cross-talks between
410 the two pathways.

411 **Complex interaction network and distributed cellular locus of actions for CMK-1 and**
412 **Calcineurin signaling**

413 Our systematic analysis of CMK-1 and calcineurin signaling cross-talks has revealed a relatively
414 complex regulatory network in which the two pathways mostly antagonize each other to regulate
415 adaptation. As mentioned above, adaptation still takes place when CMK-1 and TAX-6/CnA are
416 concomitantly inhibited, which led us to model their action as regulatory events controlling a
417 separate adaptation process (see model in Fig. 3D). While relatively complex, this model is the
418 simplest we could articulate to explain all the empirically measured interactions (see Fig.3-
419 supplement 1 for a case-by-case illustration of the proposed regulatory network functioning in
420 our different experimental conditions). In this model network, CMK-1 can regulate thermal
421 nociception via three pathways: in the first pathway CMK-1 promotes adaptation by inhibiting
422 TAX-6/CnA, which in turn inhibits adaptation. In the second and third pathways, CMK-1 works
423 independently of TAX-6/ CnA to inhibit and promote adaptation, respectively. These two latter
424 pathways can each be gated by TAX-6/ CnA. Therefore, both CMK-1 and calcineurin signaling
425 activities may promote or inhibit adaptation and shifting their activity balance could represent a
426 way to achieve nuanced yet robust modulation, integrating past activity with potentially

427 additional cues. This complex regulation scheme would be hard to achieve if the two signaling
428 pathways were working in a single neuronal cell type and it was therefore not surprising that our
429 cell-specific approaches revealed multiple cellular loci of action in the circuit controlling
430 temperature sensation and reversal execution.

431 In a previous study, CMK-1 was shown to work cell-autonomously in FLP to modulate thermo-
432 nociceptive responses following persistent noxious heat stimulation (Schild, Zbinden et al.
433 2014). FLPs are 'tonic' thermo-sensory neurons, whose activity constantly reflects the current
434 temperature (Saro, Lia et al. 2020). Here, we show that AFDs, but not FLPs, constitute the main
435 cellular locus of action of CMK-1-dependent plasticity in the case of repeated short-lasting
436 stimulations. Interestingly, AFD are mostly 'phasic' thermo-sensory neurons producing activity
437 peaks in response to thermal changes (Kimura, Miyawaki et al. 2004, Clark, Biron et al. 2006,
438 Hawk, Calvo et al. 2018, Glauser 2022). They are thus ideally suited to encode repeated thermal
439 pulses and modulate the heat-evoked reversal circuit. Laser-ablation of AFD was previously
440 shown to reduce reversal in response to head-targeted infra-red laser beams (Liu, Schulze et al.
441 2012). Here, we used thermal stimuli that were diffuse (whole animal exposure) and found that
442 neither the genetic ablation of AFD, nor the cell-specific inhibition of neurotransmission affected
443 the animal's ability to produce heat-evoked reversals. Instead, AFD was essential to favor an
444 experience-dependent reduction in heat-evoked reversal response. CMK-1 was previously
445 shown to mediate both short-term (minute timescale) and long-term (hour timescale)
446 adaptation in AFD intracellular calcium activity that resulted from thermal changes within the
447 15-25 °C innocuous temperature range (Yu, Bell et al. 2014). Long-term changes involved gene
448 expression changes, whereas the processes mediating short-term adaptation remained elusive
449 (Yu, Bell et al. 2014). At this stage, we do not know exactly how CMK-1 works in AFD to
450 orchestrate thermo-nociceptive adaptation, but we can envision many possible mechanisms,
451 including qualitative or quantitative modulation of AFD thermo-sensitivity, neuronal excitability,
452 calcium dynamics, neurotransmitter or neuro-modulator release, or even developmental effect
453 affecting AFD synaptic connectivity. Likewise, we don't know the downstream circuit involved.
454 Among different possibilities the CMK-1 signaling taking place in AFD could affect reversal via
455 AFD's direct interneuron partners AIZ and/or AIY, or engage extra-synaptic communication with
456 neuropeptides. Additional studies will thus be needed to address the downstream processes
457 that are engaged within and downstream of AFD to modulate animal responsiveness to noxious
458 heat stimuli.

459 We found that calcineurin signaling works at multiple cellular loci to control thermo-nociceptive
460 response. On the one hand, overactive TAX-6 activity in FLP is sufficient to increase reversal
461 response in naïve animals. Since FLP activity is known to favor reversal response, we might
462 hypothesize that calcineurin activity could promote FLP activity. On the other hand, overactive
463 TAX-6 activity in RIM or, to a lesser extent, in AVA/AVD/AVE neuron is sufficient to increase
464 reversal response in naïve animals, but conversely enhances reversal response upon repeated
465 stimulation. This suggests that the impact that calcineurin signaling has in these neurons
466 depends on past experience. AVA/AVD/AVE are thought to mostly promote reversal response,
467 whereas RIM neuron activity might either up-regulate, or down-regulate reversal responses
468 based on the context (Alkema, Hunter-Ensor et al. 2005, Gray, Hill et al. 2005, Guo, Hart et al.

2009, Piggott, Liu et al. 2011, Cho and Sternberg 2014, Li, Zhou et al. 2023). One particularly interesting observation is that cell-autonomous TAX-6 overactivation in interneurons acts as a major gate blocking adaptation irrespective of any CMK-1 activity manipulation. One hypothetical mechanism could be that TAX-6/CnA activity in worm would work in post-synaptic region of interneuron to adjust synaptic strength, e.g., via its action on ion channels or on inhibitory or excitatory neurotransmitter receptors, as shown in various models of synaptic plasticity in mammals (Groth, Dunbar et al. 2003).

Conclusion

In summary, our study reports the empirical identification of many potential CMK-1 targets *in vitro*, among which the catalytic subunit of Calcineurin TAX-6/CnA. Whereas we have not yet found evidence that the phosphorylation of TAX-6 by CMK-1 is directly relevant for thermo-nociceptive response modulation, we show a complex interplay between CMK-1 and calcineurin signaling that operate via multiple regulatory nodes within the noxious-heat-evoked reversal circuits of *C. elegans*. Our study paves the role for a deeper dissection of how conserved intracellular signaling pathways operating at distributed loci within a sensory-behavior circuit can actuate experience-dependent changes in nociceptive behavior.

MATERIAL AND METHODS

Worm maintenance

All *C. elegans* strains used in this study are listed in File S4. All strains were grown on nematode growth media (NGM) plates with OP50 *E. coli* (Stiernagle, 2006) at 20°C. For TAX-6 inhibition experiments, NGM plates containing cyclosporine A were used, as well as regular NGM plates as control. Cyclosporine A (10 μM) plates were prepared 72h before experiments and kept protected from light at room temperature.

Expression and purification of CMK-1(T179D)-GST, CMK-1(K52A)-GST and TAX-6-HIS6

DNA fragments encoding CMK-1 and TAX-6 proteins were PCR amplified and cloned into NdeI and BamHI restriction sites of pDK2409 (pET-24d/GST-TEV-KAP104.419C) for the GST-TEV-tagged protein and of pDK2832 (pET-24d/(His)6) for the His6-tagged proteins. Plasmids were transformed into *E. coli* BL21 (DE3) (Novagen). For protein expression, bacteria were grown overnight at 37°C, next day transferred to 200 ml of Luria Broth (LB) with kanamycin 30 μg/ml to OD_{600}=0.1, incubated up to OD_{600}=0.5. Then, protein expression was induced using 0.5 mM isopropyl β-D-1-thiogalactopyranoside (IPTG) and incubated for 5 h at 23 °C. After, bacteria cells were collected by centrifugation at 2800 rcf for 10 min at 4°C, resuspended in cold lysis buffer (150 mM NaCl, 50 mM Tris-HCl pH7.5, 1.5 mM $MgCl_2$, 5% Glycerol, 1 mM phenylmethylsulfonyl fluoride (PMSF)) and lysed in a Microfluidizer Processor M-110L. Then, NP-40 was added to the concentration of 0.1%, and soluble extract was obtained by centrifugation at 23'400 rcf for 20 min at 4 °C. Supernatant was incubated for 2 h at 4°C while rotating with Glutathione superflow beads (Qiagen) for GST-tagged CMK-1 variants or nickel-nitrilotriacetic acid beads (Ni-NTA, Qiagen) in the presence of 15 mM imidazole for TAX-6-His6 protein binding. Beads were harvested at 580 rcf at 4 °C. GST-tagged CMK-1 kinase was cleaved from the tag during incubation in lysis buffer (added 1 mM PMSF, 0.1% NP-40, 1 mM Dithiothreitol (DTT)) with home-made TEV protease. TAX-6-bound Ni-NTA beads were washed 7 times with imidazole-containing buffer (5x with 15 mM and 2x with 50 mM imidazole) and eluted in lysis buffer with 1 mM PMSF, 0.1% NP-40, 500 mM imidazole. Protein concentration was determined by Pierce Microplate BCA protein assay Kit-Reducing Agent Compatible (Thermo Scientific) using BSA as protein standard.

Total protein lysate preparation

Worms were grown on 10 cm diameter plates to the stage of young adults, washed with distilled water and suspended in extraction buffer. For *in vitro* kinase assays on peptide, urea buffer (8 M urea, 50 mM Tris-HCl pH 8.5) was used. For *in vitro* kinase assays on intact proteins, native protein extraction buffer (50 mM HEPES pH 7.4, 1% NP-40, 150 mM NaCl, 1x protease inhibitors, 0.5 mM PMSF) was used. Worms were flash-frozen in liquid nitrogen and cryogenically disrupted by using a Precellys homogenizer and acid-washed glass beads (5000 x 3 for 30 s with 30 s pause after each cycle). Lysates were collected by centrifugation at 1500 rcf at 4 °C.

In vitro kinase assay

Purified CMK-1 kinase was used the same day to avoid freezing. *In vitro* kinase assays were performed according to (Hu, Sankar et al. 2021). Briefly, for kinase assays performed on native proteins, 30 mg of worm protein extract was incubated with pre-washed NHS-activated Sepharose beads at 4°C on a rotor for 6 h. Beads were washed with 3 × 10 ml of phosphatase buffer (50 mM HEPES, 100 mM NaCl, 0.1% NP-40). 1 ml of phosphatase buffer containing 5,000 to 10,000 units of lambda phosphatase with 1 mM $MnCl_2$ was added and incubated for 4 h at room

529 temperature (RT) followed by overnight incubation at 4°C on the rotor to dephosphorylate
530 endogenous proteins. Beads were washed with 2 × 10 ml of kinase buffer (50 mM Tris-HCl pH 7.6,
531 10 mM $MgCl_2$, 150 mM NaCl and 1x PhosSTOP (Roche)). Endogenous kinases bound to beads
532 were inhibited by incubation with 1 mM FSBA in 1 ml of kinase buffer at RT on the rotor for 2 h. In
533 addition, inhibition of the remaining active kinases was achieved with a further 1 h incubation in
534 the presence of staurosporine (LC Laboratories), added to a final concentration of 100 µM. The
535 beads were washed with 3 × 10 ml of kinase buffer to remove non-bound kinase inhibitors. The
536 supernatant was removed completely using gel loading tips. Beads were split into 6 tubes (3x with
537 kinase and 1 mM ATP, 3x with kinase and without ATP (Sigma-Aldrich), kinase buffer was added
538 and incubated for 4 h at 30°C while shaking. For TAX-6 phosphorylation by CMK-1 *in vitro* assay,
539 CMK-1 was kept on Glutathione superflow beads and purified TAX-6 protein in kinase buffer (50
540 mM HEPES pH7.5, 10 mM $Mg(Ac)_2$, 1 mM DTT, 1x PhosSTOP) was added onto protein/bead mix
541 together with ATP. Afterwards samples were lyophilized followed by protein digestion using
542 trypsin. Samples were chemically labeled using dimethyl-labeling (Boersema, Raijmakers et al.
543 2009) supporting relative MS-based quantification. For kinase assays performed on peptide
544 libraries, the procedure was the same except that protein extract samples were digested with Lyc-
545 C (Lysyl Endopeptidase, WAKO) for 4 h and trypsin (Promega) overnight, before incubating them
546 with Sepharose beads. Later beads were incubated either with purified active CMK-1 or kinase
547 dead CMK-1 in kinase buffer (50 mM Tris-HCl pH 7.6, 10 mM $MgCl_2$, 150 mM NaCl, 1x PhosSTOP,
548 1 mM DTT and 1 mM γ-[^{18}O4]-ATP (Cambridge Isotope Laboratories)).

549 Peptides were fractionated and phosphopeptides enriched as described (Hu, Sankar et al. 2021);
550 briefly: samples were incubated with TiO2 (GL Sciences) slurry, which was pre-incubated with 300
551 mg/ml lactic acid in 80% acetonitrile, 1% trifluoroacetic acid (TFA) prior to enrichment for 30 min
552 at RT. For elution, TiO2 beads were transferred to 200 µl pipette tips blocked by C8 discs. After
553 washing with 10% acetonitrile/1% TFA, 80% acetonitrile/1% TFA, and LC-MS grade water,
554 phosphopeptides were eluted with 1.25% ammonia in 20% acetonitrile and 1.25% ammonia in
555 80% acetonitrile. Eluates were acidified with formic acid, concentrated by vacuum concentration,
556 and resuspended in 0.1% formic acid for LC-MS/MS analysis.

557 ***LC-MS/MS analyses***

558 LC-MS/MS measurements were performed on two LC-MS/MS systems as described (Hu, Sankar
559 et al. 2021): a QExactive (QE) Plus and HF-X mass spectrometer coupled to an EasyLC 1000 and
560 EasyLC 1200 nanoflow-HPLC, respectively (all Thermo Scientific). Peptides were fractionated on
561 fused silica HPLC-column tips using a gradient of A (0.1% formic acid in water) and B (0.1% formic
562 acid in 80% acetonitrile in water): 5%–30% B within 85 min with a flow rate of 250 nl/min. Mass
563 spectrometers were operated in the data-dependent mode; after each MS scan (m/z = 370 – 1750;
564 resolution: 70'000 for QE Plus and 120'000 for HF-X) a maximum of ten, or twelve MS/MS scans
565 were performed (normalized collision energy of 25%), a target value of 1'000 (QE Plus)/5'000 (HF-
566 X) and a resolution of 17'500 for QE Plus and 30'000 for HF-X. MS raw files were analyzed using
567 MaxQuant (version 1.6.2.10) (Cox and Mann 2008) using a full-length *C. elegans* Uniprot database
568 (November, 2017), and common contaminants such as keratins and enzymes used for in-gel
569 digestion as reference. Carbamidomethylcysteine was set as fixed modification and protein
570 amino-terminal acetylation, serine-, threonine- and tyrosine- (heavy) phosphorylation, and
571 oxidation of methionine were set as variable modifications. In case of labeled samples, triple
572 dimethyl-labeling was chosen as quantification method (Boersema, Raijmakers et al. 2009). The
573 MS/MS tolerance was set to 20 ppm and three missed cleavages were allowed using trypsin/P as
574 enzyme specificity. Peptide, site, and protein FDR based on a forward-reverse database were set

575 to 0.01, minimum peptide length was set to 7, the minimum score for modified peptides was 40,
576 and minimum number of peptides for identification of proteins was set to one, which must be
577 unique. The "match-between-run" option was used with a time window of 0.7 min. MaxQuant
578 results were analyzed using Perseus (Tyanova, Temu et al. 2016).

579 **Worm preparation for heat avoidance assay and number of replicates**

580 Gravid adult worms were treated with hypochlorite solution according to standard protocol.
581 Embryos were rinsed twice with water and once with M9 buffer, then resuspended in M9 and
582 plated on NGM plates seeded with OP-50 *E. coli*. 200-300 embryos per individual plate were
583 seeded. Worms were incubated at 20°C until start of egg laying (65-90 h, depending on the strain
584 or condition). Worms were washed off the plates with distilled water, placed into 1.5 ml tubes and
585 washed twice more to remove bacterial residues. Worms were placed on unseeded NGM plates
586 and left to disperse and acclimate in the experimental room for 60 min. Prior to worm deposition,
587 these experimental unseeded plates were kept open in a laminar flow hood for 3 h to ensure dry
588 surface. Plate lid was removed 3 min before starting the assay. At least 3 replicates were
589 performed for each strain or condition on 3 separate days running wild-type N2 strain alongside.

590 For the experiments using transgenic animals, fluorescent signal-carrying worms were picked 16-
591 19 h before the experiment to allow for recovery.

592 **Heat stimulation and adaptation protocols**

593 For the majority of experiments, we compared the heat-evoked response in naïve animals (that
594 had never been stimulated, T0) and the same animals after 60 minutes of repeated stimulation
595 (4-s stimuli and 20s interstimulus interval (ISI), T60). For some experiments, the adaptation period
596 was reduced to 10 min (T10) or 30 min (T30). The INFERNO system (Lia and Glauser 2020) was
597 used for behavioral recordings. The heat stimulation program during recordings was composed of
598 a 40-s baseline period without any heat stimulation, a 4-s stimulation with 400 W heating (4 IR
599 lamps turned on) and a 20-s post stimulation period. The repeated stimulation delivery
600 (adaptation treatment) was achieved by placing the worm plates under the ThermINATOR system
601 (Lia and Glauser 2020), providing infinitely looping temperature program composed of 4 s of IR
602 lamps stimulation, followed by 20 s ISI with the lamps turned off. There was a lag of about 10 s for
603 the plate transfer between the two systems.

604 In the INFERNO system, worm plates were recorded using a DMK 33U×250 camera and movies
605 acquired with the IC capture software (The Imaging Source), at 8 frames per second, at a
606 1600×1800 pixel resolution, and the resulting .AVI file was encoded as Y800 8-bit monochrome.
607 The Multi-Worm Tracker 1.3.0 (MWT) (Swierczek, Giles et al. 2011) with previously described
608 configuration settings (Lia and Glauser 2020) was used for movie analyses. A previously described
609 Python script was use to flag the frame of reversal occurrence (Lia and Glauser 2020). Each
610 reported data point corresponds to the results of one assay plate scoring at least 50 animals.

611 **Transgene construction and transgenesis**

612 Promoter-containing Entry plasmids (Multi-site Gateway slot 1) were constructed by PCR using
613 N2 genomic DNA as template and primers flanked by attB4 and attB1r recombination sites; the
614 PCR product being cloned into pDONR-P4-P1R vector (Invitrogen) by BP recombination.

615 Coding sequence-containing Entry plasmids (Multi-site Gateway slot 2) were constructed by PCR
616 using N2 cDNA as template and primers flanked by attB1 and attB2 recombination sites; the PCR
617 product being cloned into pDONR_221 vector (Invitrogen) by BP recombination.

618 Expression plasmids for transgenesis were created through a LR recombination reaction
619 (Gateway™ LR Clonase, Invitrogen) as per the manufacturer's instructions.

620 Primer sequences for BP reactions and all plasmids used in this study are listed in File S4.

621 DNA constructs were transformed into competent DH5a *E. coli* (NEB C2987H), purified with the
622 GenElute HP Plasmid miniprep kit (Sigma) and microinjected in the worm gonad according to a
623 standard protocol (Evans 2006) together with co-injection markers for transgenic animal
624 identification. The concentrations of expression plasmids and co-markers injected are indicated
625 in File S4.

626 **Site-directed mutagenesis**

627 To create truncated *tax-6(gf)* transgene PCR-based site-directed mutagenesis (Hemsley, Arnheim
628 et al. 1989) was used. Entry plasmid containing *tax-6* coding DNA sequence was amplified with
629 the KOD Hot Start DNA Polymerase (Novagen; Merck). Primers were designed to contain the
630 desired deletion and phosphorylated in 5' end (File S4). Linear PCR products were purified from
631 agarose gel (1%) after electrophoresis with a Zymoclean-Gel DNA Recovery kit (Zymo Research),
632 circularized using DNA Ligation Kit <Mighty Mix> (Takara).

633 **Statistical analyses**

634 ANOVAs were conducted using Jamovi (The jamovi project (2022), jamovi (Version 2.3) [Computer
635 Software]; retrieved from (https://www.jamovi.org). Post hoc tests were used to compare each of
636 the mutants with wild type (N2) or *cmk-1(lf)* using Bonferroni–Holm correction.

637

638 **DATA AVAILABILITY**

639 MS data have been deposited to the ProteomeXchange Consortium via the PRIDE partner
640 repository with the dataset identifier PXD055776 (Perez-Riverol, Bai et al. 2022). The raw data and
641 *p* values presented in the different figures are provided in File S3.

642

643 **ACKNOWLEDGEMENTS**

644 We are grateful to Lisa Schild, Laurence Bulliard and Michael Stumpe for expert technical
645 support. Some strains were provided by the CGC, which is funded by NIH Office of Research
646 Infrastructure Programs (P40 OD010440). The study was supported by the Swiss National
647 Science Foundation (BSSGI0_155764, PP00P3_150681, and 310030_197607 to DAG,
648 310030_212187 to JD) and by the Novartis Foundation for Medical-Biological Research.

649

650 **COMPETING INTERESTS**

651 No competing interests declared

652

653

REFERENCES

Alkema, M. J., M. Hunter-Ensor, N. Ringstad and H. R. Horvitz (2005). "Tyramine Functions independently of octopamine in the Caenorhabditis elegans nervous system." Neuron **46**(2): 247-260.

Amna, K., K. Salman and K. Yeong Shik (2019). "Insight into Pain Modulation: Nociceptors Sensitization and Therapeutic Targets." Current Drug Targets **20**(7): 775-788.

Ardiel, E. L., T. A. McDiarmid, T. A. Timbers, K. C. Y. Lee, J. Safaei, S. L. Pelech and C. H. Rankin (2018). "Insights into the roles of CMK-1 and OGT-1 in interstimulus interval-dependent habituation in Caenorhabditis elegans." **285**(1891): 20182084.

Bandyopadhyay, J., J. Lee and A. Bandyopadhyay (2004). "Regulation of calcineurin, a calcium/calmodulin-dependent protein phosphatase, in C. elegans." Mol Cells **18**(1): 10-16.

Bandyopadhyay, J., J. Lee, J. Lee, J. I. Lee, J. R. Yu, C. Jee, J. H. Cho, S. Jung, M. H. Lee, S. Zannoni, A. Singson, D. H. Kim, H. S. Koo and J. Ahnn (2002). "Calcineurin, a calcium/calmodulin-dependent protein phosphatase, is involved in movement, fertility, egg laying, and growth in Caenorhabditis elegans." Mol Biol Cell **13**(9): 3281-3293.

Basith, S., M. Cui, S. Hong and S. Choi (2016). "Harnessing the Therapeutic Potential of Capsaicin and Its Analogues in Pain and Other Diseases." Molecules (Basel, Switzerland) **21**(8): 966.

Boersema, P. J., R. Raijmakers, S. Lemeer, S. Mohammed and A. J. Heck (2009). "Multiplex peptide stable isotope dimethyl labeling for quantitative proteomics." Nat Protoc **4**(4): 484-494.

Breimhorst, M., M. Hondrich, C. Rebhorn, A. May and F. Birklein (2012). "Sensory and sympathetic correlates of heat pain sensitization and habituation in men and women." Eur J Pain **16**(9): 1281-1292.

Brockie, P. J., J. E. Mellem, T. Hills, D. M. Madsen and A. V. Maricq (2001). "The C. elegans glutamate receptor subunit NMR-1 is required for slow NMDA-activated currents that regulate reversal frequency during locomotion." Neuron **31**(4): 617-630.

Byrne Rodgers, J. and W. S. Ryu (2020). "Targeted thermal stimulation and high-content phenotyping reveal that the C. elegans escape response integrates current behavioral state and past experience." PLOS ONE **15**(3): e0229399.

Calalb, M. B., R. L. Kincaid and T. R. Soderling (1990). "Phosphorylation of calcineurin: Effect on calmodulin binding." Biochemical and Biophysical Research Communications **172**(2): 551-556.

Chatzigeorgiou, M. and William R. Schafer (2011). "Lateral Facilitation between Primary Mechanosensory Neurons Controls Nose Touch Perception in C. elegans." Neuron **70**(2): 299-309.

Chatzigeorgiou, M., S. Yoo, J. D. Watson, W. H. Lee, W. C. Spencer, K. S. Kindt, S. W. Hwang, D. M. Miller, 3rd, M. Treinin, M. Driscoll and W. R. Schafer (2010). "Specific roles for DEG/ENaC and TRP channels in touch and thermosensation in C. elegans nociceptors." Nat Neurosci **13**(7): 861-868.

Cho, J. Y. and P. W. Sternberg (2014). "Multilevel modulation of a sensory motor circuit during C. elegans sleep and arousal." Cell **156**(1-2): 249-260.

Clark, D. A., D. Biron, P. Sengupta and A. D. Samuel (2006). "The AFD sensory neurons encode multiple functions underlying thermotactic behavior in Caenorhabditis elegans." J Neurosci **26**(28): 7444-7451.

Corcoran, E. E., J. D. Joseph, J. A. MacDonald, C. D. Kane, T. A. J. Haystead and A. R. Means (2003). "Proteomic Analysis of Calcium/Calmodulin-dependent Protein Kinase I and IV in Vitro Substrates Reveals Distinct Catalytic Preferences*." Journal of Biological Chemistry **278**(12): 10516-10522.

Cox, J. and M. Mann (2008). "MaxQuant enables high peptide identification rates, individualized p.p.b.-range mass accuracies and proteome-wide protein quantification." Nat Biotechnol **26**(12): 1367-1372.

Dai, F., C. Hu, X. Li, Z. Zhang, H. Wang, W. Zhou, J. Wang, Q. Geng, Y. Dong and C. Tang (2024). "Cav3.2 channel regulates cerebral ischemia/reperfusion injury: a promising target for intervention." Neural Regen Res **19**(11): 2480-2487.

de Tommaso, M., A. Federici, R. Santostasi, R. Calabrese, E. Vecchio, G. Lapadula, F. Iannone, P. Lamberti and P. Livrea (2011). "Laser-Evoked Potentials Habituation in Fibromyalgia." The Journal of Pain **12**(1): 116-124.

de Tommaso, M., L. Lo Sito, O. Di Fruscolo, M. Sardaro, M. Pia Prudenzano, P. Lamberti and P. Livrea (2005). "Lack of habituation of nociceptive evoked responses and pain sensitivity during migraine attack." Clin Neurophysiol **116**(6): 1254-1264.

Dubin, A. E. and A. Patapoutian (2010). "Nociceptors: the sensors of the pain pathway." J Clin Invest **120**(11): 3760-3772.

Eto, K., N. Takahashi, Y. Kimura, Y. Masuho, K. Arai, M. A. Muramatsu and H. Tokumitsu (1999). "Ca(2+)/Calmodulin-dependent protein kinase cascade in Caenorhabditis elegans. Implication in transcriptional activation." J Biol Chem **274**(32): 22556-22562.

Evans, T. C., (ed) (2006). "Transformation and microinjection." WormBook.

Fu, Y., J. Han, T. Ishola, M. Scerbo, H. Adwanikar, C. Ramsey and V. Neugebauer (2008). "PKA and ERK, but not PKC, in the amygdala contribute to pain-related synaptic plasticity and behavior." Mol Pain **4**: 26.

Gillis, A. M., K. M. Kavanagh, H. J. Mathison, J. R. Somers, S. Zhan and H. J. Duff (2004). "Heart block in mice overexpressing calcineurin but not NF-AT3." Cardiovasc Res **64**(3): 488-495.

Glauser, D. A. (2022). "Temperature sensing and context-dependent thermal behavior in nematodes." Curr Opin Neurobiol **73**: 102525.

Glauser, D. A., W. C. Chen, R. Agin, B. L. Macinnis, A. B. Hellman, P. A. Garrity, M. W. Tan and M. B. Goodman (2011). "Heat avoidance is regulated by transient receptor potential (TRP) channels and a neuropeptide signaling pathway in Caenorhabditis elegans." Genetics **188**(1): 91-103.

Gooch, J. L., J. J. Toro, R. L. Guler and J. L. Barnes (2004). "Calcineurin A-alpha but not A-beta is required for normal kidney development and function." Am J Pathol **165**(5): 1755-1765.

Gray, J. M., J. J. Hill and C. I. Bargmann (2005). "A circuit for navigation in Caenorhabditis elegans." Proc Natl Acad Sci U S A **102**(9): 3184-3191.

Groth, R. D., R. L. Dunbar and P. G. Mermelstein (2003). "Calcineurin regulation of neuronal plasticity." Biochemical and Biophysical Research Communications **311**(4): 1159-1171.

Guo, Z. V., A. C. Hart and S. Ramanathan (2009). "Optical interrogation of neural circuits in Caenorhabditis elegans." Nat Methods **6**(12): 891-896.

Harris, N., S. G. Bates, Z. Zhuang, M. Bernstein, J. M. Stonemetz, T. J. Hill, Y. V. Yu, J. A. Calarco and P. Sengupta (2023). "Molecular encoding of stimulus features in a single sensory neuron type enables neuronal and behavioral plasticity." Current Biology **33**(8): 1487-1501.e1487.

Hashimoto, Y., M. M. King and T. R. Soderling (1988). "Regulatory interactions of calmodulin-binding proteins: phosphorylation of calcineurin by autophosphorylated Ca2+/calmodulin-dependent protein kinase II." Proc Natl Acad Sci U S A **85**(18): 7001-7005.

Hashimoto, Y. and T. R. Soderling (1989). "Regulation of calcineurin by phosphorylation. Identification of the regulatory site phosphorylated by Ca2+/calmodulin-dependent protein kinase II and protein kinase C." J Biol Chem **264**(28): 16524-16529.

Hawk, J. D., A. C. Calvo, P. Liu, A. Almoril-Porras, A. Aljobeh, M. L. Torruella-Suarez, I. Ren, N. Cook, J. Greenwood, L. Luo, Z. W. Wang, A. D. T. Samuel and D. A. Colon-Ramos (2018). "Integration of Plasticity Mechanisms within a Single Sensory Neuron of C. elegans Actuates a Memory." Neuron **97**(2): 356-367.e354.

Hemsley, A., N. Arnheim, M. D. Toney, G. Cortopassi and D. J. Galas (1989). "A simple method for site-directed mutagenesis using the polymerase chain reaction." Nucleic acids research **17**(16): 6545-6551.

Hilliard, M. A., A. J. Apicella, R. Kerr, H. Suzuki, P. Bazzicalupo and W. R. Schafer (2005). "In vivo imaging of C. elegans ASH neurons: cellular response and adaptation to chemical repellents." EMBO J **24**(1): 63-72.

Hu, Z., D. S. Sankar, B. Vu, A. Leytens, C. Vionnet, W. Wu, M. Stumpe, E. Martínez-Martínez, B. Stork and J. Dengjel (2021). "ULK1 phosphorylation of striatin activates protein phosphatase 2A and autophagy." Cell Rep **36**(13): 109762.

Huang, Y., S.-R. Chen, H. Chen, Y. Luo and H.-L. Pan (2020). "Calcineurin Inhibition Causes α2δ-1–Mediated Tonic Activation of Synaptic NMDA Receptors and Pain Hypersensitivity." **40**(19): 3707-3719.

Huang, Y., S.-R. Chen and H.-L. Pan (2022). "Calcineurin Regulates Synaptic Plasticity and Nociceptive Transmission at the Spinal Cord Level." **28**(6): 628-638.

Isensee, J., M. Diskar, S. Waldherr, R. Buschow, J. Hasenauer, A. Prinz, F. Allgöwer, F. W. Herberg and T. Hucho (2014). "Pain modulators regulate the dynamics of PKA-RII phosphorylation in subgroups of sensory neurons." Journal of Cell Science **127**(1): 216-229.

Johnson, J. L., T. M. Yaron, E. M. Huntsman, A. Kerelsky, J. Song, A. Regev, T.-Y. Lin, K. Liberatore, D. M. Cizin, B. M. Cohen, N. Vasan, Y. Ma, K. Krismer, J. T. Robles, B. van de Kooij, A. E. van Vlimmeren, N. Andrée-Busch, N. F. Käufer, M. V. Dorovkov, A. G. Ryazanov, Y. Takagi, E. R. Kastenhuber, M. D. Goncalves,

B. D. Hopkins, O. Elemento, D. J. Taatjes, A. Maucuer, A. Yamashita, A. Degterev, M. Uduman, J. Lu, S. D. Landry, B. Zhang, I. Cossentino, R. Linding, J. Blenis, P. V. Hornbeck, B. E. Turk, M. B. Yaffe and L. C. Cantley (2023). "An atlas of substrate specificities for the human serine/threonine kinome." Nature **613**(7945): 759-766.

Jordan, A. and D. A. Glauser (2023). "Distinct clusters of human pain gene orthologs in Caenorhabditis elegans regulate thermo-nociceptive sensitivity and plasticity." Genetics **224**(1).

Kaplan, J. M. and H. R. Horvitz (1993). "A dual mechanosensory and chemosensory neuron in Caenorhabditis elegans." Proc Natl Acad Sci U S A **90**(6): 2227-2231.

Ke, C., Y. Huang, Z. Mao, Z. Ke, Z. Wang, R. Li, S. Long, Y. Guo, F. Wang, M. Qian, R. Zhao, J. Zheng and S. Xie (2023). "Calcineurin suppresses rat H9c2 cardiomyocyteprotective autophagy under chronic intermittent hypoxia by downregulating the AMPK pathway." Exp Cell Res **433**(2): 113850.

Kidd, B. L. and L. A. Urban (2001). "Mechanisms of inflammatory pain." BJA: British Journal of Anaesthesia **87**(1): 3-11.

Kimura, K. D., A. Miyawaki, K. Matsumoto and I. Mori (2004). "The C. elegans Thermosensory Neuron AFD Responds to Warming." Current Biology **14**(14): 1291-1295.

Kimura, Y., E. E. Corcoran, K. Eto, K. Gengyo-Ando, M.-a. Muramatsu, R. Kobayashi, J. H. Freedman, S. Mitani, M. Hagiwara, A. R. Means and H. Tokumitsu (2002). "A CaMK cascade activates CRE-mediated transcription in neurons of Caenorhabditis elegans." EMBO Rep **3**(10): 962-966.

Klee, C. B., T. H. Crouch and M. H. Krinks (1979). "Calcineurin: a calcium- and calmodulin-binding protein of the nervous system." Proc Natl Acad Sci U S A **76**(12): 6270-6273.

Kotera, I., N. A. Tran, D. Fu, J. H. Kim, J. Byrne Rodgers and W. S. Ryu (2016). "Pan-neuronal screening in Caenorhabditis elegans reveals asymmetric dynamics of AWC neurons is critical for thermal avoidance behavior." eLife **5**: e19021.

Kuhara, A., H. Inada, I. Katsura and I. Mori (2002). "Negative Regulation and Gain Control of Sensory Neurons by the C. elegans Calcineurin TAX-6." Neuron **33**(5): 751-763.

Kuner, R. and H. Flor (2017). "Structural plasticity and reorganisation in chronic pain." Nature Reviews Neuroscience **18**(1): 20-30.

Lee, J., C. Jee, H. O. Song, J. Bandyopadhyay, J. I. Lee, J. R. Yu, J. Lee, B. J. Park and J. Ahnn (2004). "Opposing functions of calcineurin and CaMKII regulate G-protein signaling in egg-laying behavior of C.elegans." J Mol Biol **344**(2): 585-595.

Lee, J., H. O. Song, C. Jee, L. Vanoaica and J. Ahnn (2005). "Calcineurin regulates enteric muscle contraction through EXP-1, excitatory GABA-gated channel, in C. elegans." J Mol Biol **352**(2): 313-318.

Lee, J. C., Y. G. Kwon, D. S. Lawrence and A. M. Edelman (1994). "A requirement of hydrophobic and basic amino acid residues for substrate recognition by Ca2+/calmodulin-dependent protein kinase Ia." Proc Natl Acad Sci U S A **91**(14): 6413-6417.

Lemieux, George A., Katherine A. Cunningham, L. Lin, F. Mayer, Z. Werb and K. Ashrafi (2015). "Kynurenic Acid Is a Nutritional Cue that Enables Behavioral Plasticity." Cell **160**(1): 119-131.

Li, W., L. Kang, B. J. Piggott, Z. Feng and X. Z. S. Xu (2011). "The neural circuits and sensory channels mediating harsh touch sensation in Caenorhabditis elegans." Nat Commun **2**: 315.

Li, Z., J. Zhou, K. A. Wani, T. Yu, E. A. Ronan, B. J. Piggott, J. Liu and X. Z. S. Xu (2023). "A C. elegans neuron both promotes and suppresses motor behavior to fine tune motor output." **16**.

Lia, A.-S. and D. A. Glauser (2020). "A system for the high-throughput analysis of acute thermal avoidance and adaptation in C. elegans." J Biol Methods.

Liang, R. J., X. L. Liu, L. M. Wei, W. Wang, P. Zheng, X. S. Yan, Y. L. Zhao, L. J. Liu and X. H. Cao (2012). "The modulation of the excitability of primary sensory neurons by Ca2+-CaM-CaMKII pathway." Neurological Sciences **33**(5): 1083-1093.

Lim, J. P., H. Fehlauer, A. Das, G. Saro, D. A. Glauser, A. Brunet and M. B. Goodman (2018). "Loss of CaMKI Function Disrupts Salt Aversive Learning in C. elegans." J Neurosci **38**(27): 6114-6129.

Liu, J., J. D. Farmer, Jr., W. S. Lane, J. Friedman, I. Weissman and S. L. Schreiber (1991). "Calcineurin is a common target of cyclophilin-cyclosporin A and FKBP-FK506 complexes." Cell **66**(4): 807-815.

Liu, S., E. Schulze and R. Baumeister (2012). "Temperature- and Touch-Sensitive Neurons Couple CNG and TRPV Channel Activities to Control Heat Avoidance in Caenorhabditis elegans." PLoS One **7**(3): e32360.

May, A., R. Rodriguez-Raecke, A. Schulte, K. Ihle, M. Breimhorst, F. Birklein and T. P. Jürgens (2012). "Within-session sensitization and between-session habituation: A robust physiological response to repetitive painful heat stimulation." European Journal of Pain **16**(3): 401-409.

Molkentin, J. D. (2004). "Calcineurin-NFAT signaling regulates the cardiac hypertrophic response in coordination with the MAPKs." Cardiovasc Res **63**(3): 467-475.

Moss, B. J., L. Park, C. L. Dahlberg and P. Juo (2016). "The CaM Kinase CMK-1 Mediates a Negative Feedback Mechanism Coupling the C. elegans Glutamate Receptor GLR-1 with Its Own Transcription." PLoS Genet **12**(7): e1006180.

Mukherjee, A. and C. Soto (2011). "Role of calcineurin in neurodegeneration produced by misfolded proteins and endoplasmic reticulum stress." Curr Opin Cell Biol **23**(2): 223-230.

Neal, S. J., A. Takeishi, M. P. O'Donnell, J. Park, M. Hong, R. A. Butcher, K. Kim and P. Sengupta (2015). "Feeding state-dependent regulation of developmental plasticity via CaMKI and neuroendocrine signaling." eLife **4**: e10110.

Nkambeu, B., J. B. Salem and F. Beaudry (2020). "Capsaicin and Its Analogues Impede Nocifensive Response of Caenorhabditis elegans to Noxious Heat." Neurochem Res **45**(8): 1851-1859.

O'Neill, J., C. Brock, A. E. Olesen, T. Andresen, M. Nilsson and A. H. Dickenson (2012). "Unravelling the mystery of capsaicin: a tool to understand and treat pain." Pharmacological reviews **64**(4): 939-971.

Pace, M. C., M. B. Passavanti, L. De Nardis, F. Bosco, P. Sansone, V. Pota, M. Barbarisi, A. Palagiano, F. A. Iannotti, E. Panza and C. Aurilio (2018). "Nociceptor plasticity: A closer look." Journal of Cellular Physiology **233**(4): 2824-2838.

Perez-Riverol, Y., J. Bai, C. Bandla, D. García-Seisdedos, S. Hewapathirana, S. Kamatchinathan, D. J. Kundu, A. Prakash, A. Frericks-Zipper, M. Eisenacher, M. Walzer, S. Wang, A. Brazma and J. A. Vizcaíno (2022). "The PRIDE database resources in 2022: a hub for mass spectrometry-based proteomics evidences." Nucleic Acids Res **50**(D1): D543-d552.

Peuker, K., A. Strigli, D. V. F. Tauriello, A. Hendricks, W. von Schönfels, G. Burmeister, M. Brosch, A. Herrmann, S. Krüger, J. Nitsche, L. Južnić, M. M. Geissler, A. Hiergeist, A. Gessner, J. Wirbel, R. P. Ponnudurai, A. Tunger, R. Wehner, D. E. Stange, J. Weitz, D. E. Aust, G. B. Baretton, M. Schmitz, C. Röcken, J. Hampe, S. Hinz, G. Zeller, T. Chavakis, C. Schafmayer, E. Batlle and S. Zeissig (2022). "Microbiota-dependent activation of the myeloid calcineurin-NFAT pathway inhibits B7H3- and B7H4-dependent anti-tumor immunity in colorectal cancer." Immunity **55**(4): 701-717.e707.

Piggott, B. J., J. Liu, Z. Feng, S. A. Wescott and X. Z. Xu (2011). "The neural circuits and synaptic mechanisms underlying motor initiation in C. elegans." Cell **147**(4): 922-933.

Rodriguez-Raecke, R., B. Doganci, M. Breimhorst, A. Stankewitz, C. Buchel, F. Birklein and A. May (2010). "Insular cortex activity is associated with effects of negative expectation on nociceptive long-term habituation." J Neurosci **30**(34): 11363-11368.

Rusnak, F. and P. Mertz (2000). "Calcineurin: form and function." Physiol Rev **80**(4): 1483-1521.

Sandkühler, J. (2009). "Models and Mechanisms of Hyperalgesia and Allodynia." Physiological Reviews **89**(2): 707-758.

Saro, G., A. S. Lia, S. Thapliyal, F. Marques, K. E. Busch and D. A. Glauser (2020). "Specific Ion Channels Control Sensory Gain, Sensitivity, and Kinetics in a Tonic Thermonociceptor." Cell Rep **30**(2): 397-408 e394.

Sato, Y., T. Onaka, E. Kobayashi and N. Seo (2007). "The differential effect of cyclosporine on hypnotic response and pain reaction in mice." Anesth Analg **105**(5): 1489-1493, table of contents.

Satterlee, J. S., W. S. Ryu and P. Sengupta (2004). "The CMK-1 CaMKI and the TAX-4 Cyclic nucleotide-gated channel regulate thermosensory neuron gene expression and function in C. elegans." Curr Biol **14**(1): 62-68.

Schild, Lisa C., L. Zbinden, Harold W. Bell, Yanxun V. Yu, P. Sengupta, Miriam B. Goodman and Dominique A. Glauser (2014). "The Balance between Cytoplasmic and Nuclear CaM Kinase-1 Signaling Controls the Operating Range of Noxious Heat Avoidance." Neuron **84**(5): 983-996.

Shum, F. W. F., S. W. Ko, Y.-S. Lee, B.-K. Kaang and M. Zhuo (2005). "Genetic alteration of anxiety and stress-like behavior in mice lacking CaMKIV." Molecular Pain **1**(1): 22.

Smith, B. W., E. M. Tooley, E. Q. Montague, A. E. Robinson, C. J. Cosper and P. G. Mullins (2008). "Habituation and sensitization to heat and cold pain in women with fibromyalgia and healthy controls." PAIN **140**(3): 420-428.

Smith, H. S. (2009). "Calcineurin as a nociceptor modulator." Pain Physician **12**(4): E309-318.

Swierczek, N. A., A. C. Giles, C. H. Rankin and R. A. Kerr (2011). "High-throughput behavioral analysis in C. elegans." Nat Methods **8**(7): 592-598.

Thapliyal, S., I. Beets and D. A. Glauser (2023). "Multisite regulation integrates multimodal context in sensory circuits to control persistent behavioral states in C. elegans." Nature Communications **14**(1): 3052.

Treede, R. D. (1995). "Peripheral acute pain mechanisms." Ann Med **27**(2): 213-216.

Tyanova, S., T. Temu, P. Sinitcyn, A. Carlson, M. Y. Hein, T. Geiger, M. Mann and J. Cox (2016). "The Perseus computational platform for comprehensive analysis of (prote)omics data." Nat Methods **13**(9): 731-740.

Wang, H., Y. Du, B. Xiang, W. Lin, X. Li and Q. Wei (2008). "A renewed model of CNA regulation involving its C-terminal regulatory domain and CaM." Biochemistry **47**(15): 4461-4468.

Wang, H. and M. Zhang (2012). The role of Ca2+-stimulated adenylyl cyclases in bidirectional synaptic plasticity and brain function. Reviews in the Neurosciences. **23:** 67.

White, R. R., Y. G. Kwon, M. Taing, D. S. Lawrence and A. M. Edelman (1998). "Definition of optimal substrate recognition motifs of Ca2+-calmodulin-dependent protein kinases IV and II reveals shared and distinctive features." J Biol Chem **273**(6): 3166-3172.

Willis Jr., W. D. (2001). "Role of Neurotransmitters in Sensitization of Pain Responses." Annals of the New York Academy of Sciences **933**(1): 142-156.

Wittenburg, N. and R. Baumeister (1999). "Thermal avoidance in Caenorhabditis elegans: an approach to the study of nociception." Proc Natl Acad Sci U S A **96**(18): 10477-10482.

Yu, Y. V., H. W. Bell, D. Glauser, S. D. Van Hooser, M. B. Goodman and P. Sengupta (2014). "CaMKI-dependent regulation of sensory gene expression mediates experience-dependent plasticity in the operating range of a thermosensory neuron." Neuron **84**(5): 919-926.

Yuan, Y. P., Z. Y. Shen, T. Teng, S. C. Xu, C. Y. Kong, X. F. Zeng, A. H. B. M and L. Yan (2024). "S100a8/9 (S100 Calcium Binding Protein a8/9) Promotes Cardiac Hypertrophy Via Upregulation of FGF23 (Fibroblast Growth Factor 23) in Mice." J Am Heart Assoc **13**(10): e028006.

Zhou, Y.-Q., D.-Q. Liu, S.-P. Chen, J. Sun, X.-R. Zhou, F. Luo, Y.-K. Tian and D.-W. Ye (2017). "Cellular and Molecular Mechanisms of Calcium/Calmodulin-Dependent Protein Kinase II in Chronic Pain." Journal of Pharmacology and Experimental Therapeutics **363**(2): 176.

901 **FIGURES AND LEGENDS**

902

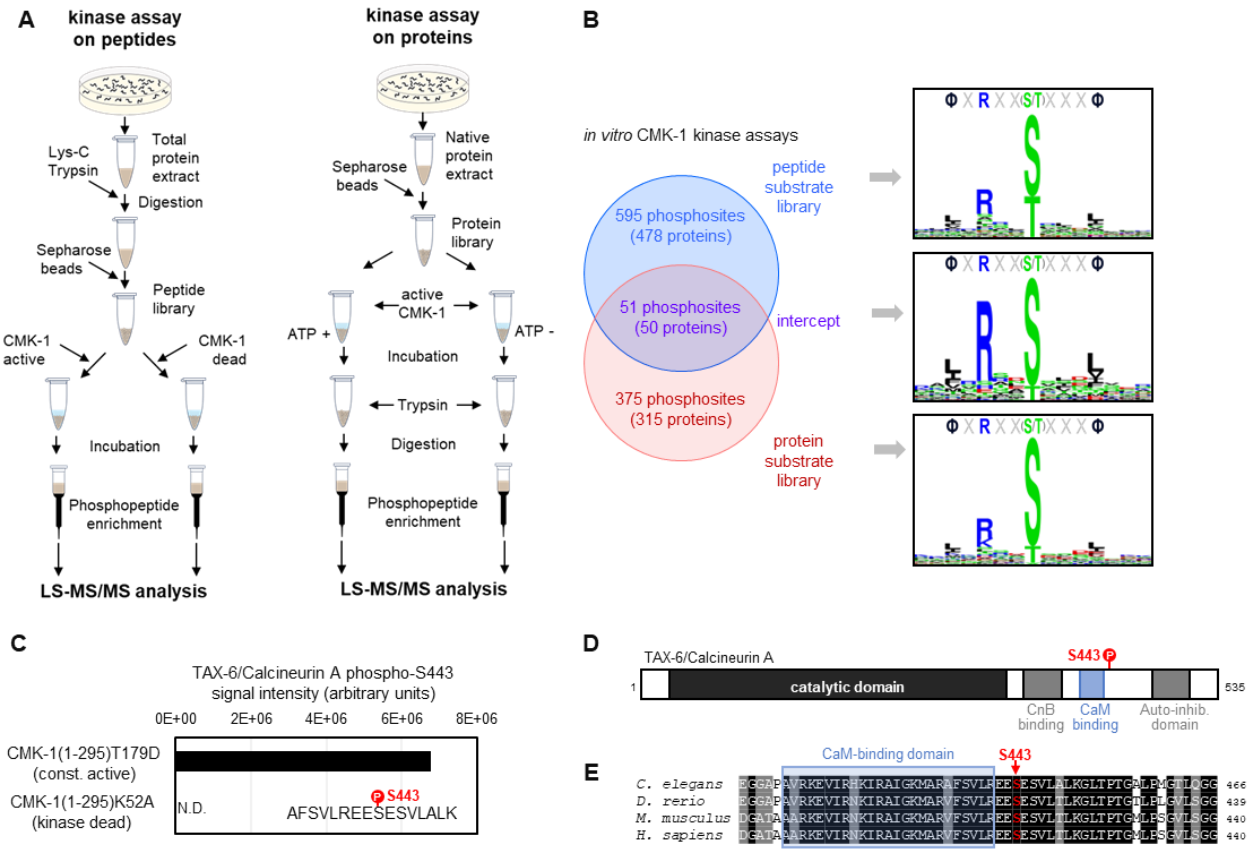

903

904 **Figure 1 Identification of CMK-1 phosphorylation substrates**

905 **A**. Schematic of the two approaches used for the large-scale identification of the CMK-1
906 phosphorlyation substrates *in vitro*. *In vitro* kinase assays using a *C. elegans* peptide library (left)
907 or a *C. elegans* native protein library (right) were followed by MS-based phosphoproteomics
908 analyses. The activity of a constitutively active mutant (CMK-1(1-295)T179D) was compared to
909 control situations with either kinase dead mutant (CMK-1(1-295)K52A) or without ATP co-
910 substrate during the incubation. **B**. Comparison of the results with the two approaches, showing
911 the number of overlapping and non-overlapping phosphosites, the number of corresponding
912 proteins, as well as the 15-residue consensus sequence surrounding the phosphosites. Logos
913 created with Seq2Logo. **C**. Results of a separate *in vitro* kinase assay in which purified TAX-
914 6/CnA was used as substrate and showing TAX-6/CnA S443 phosphorylation. N.D., not detected
915 **D**. Diagram presenting the different regions of the *C. elegans* TAX6/CnA protein and the
916 localization of S443. **E**. Alignments showing high conservation of a CnA protein region around
917 S443 across *C. elegans, Danio rerio, Mus Musculus* and *Homo sapiens* (Uniprot assessions:
918 Q0G819-2|PP2B_CAEEL; A3KGZ6|A3KGZ6_DANRE; P63328|PP2BA_MOUSE;
919 Q08209|PP2BA_HUMAN).

920

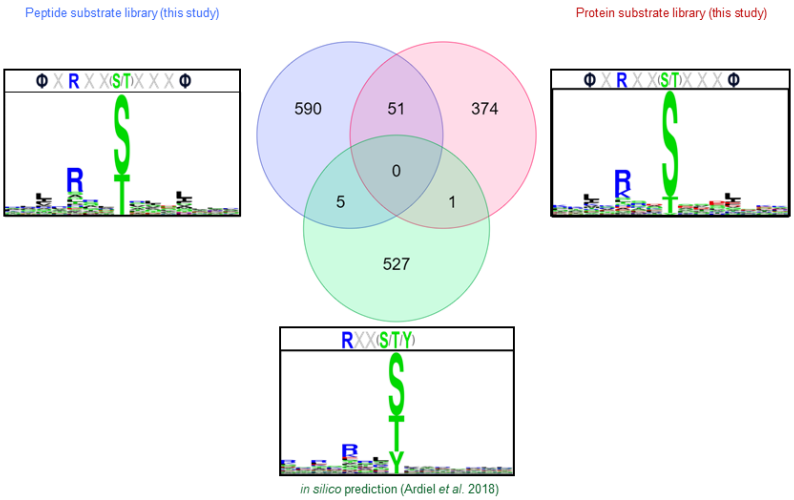

Figure 1 -supplement 1 Comparison of empirically identified CMK-1 phospho-substrates with previously published predictions

Venn diagram showing the number of phosphosites from the indicated lists and the consensus as in Fig. 1.

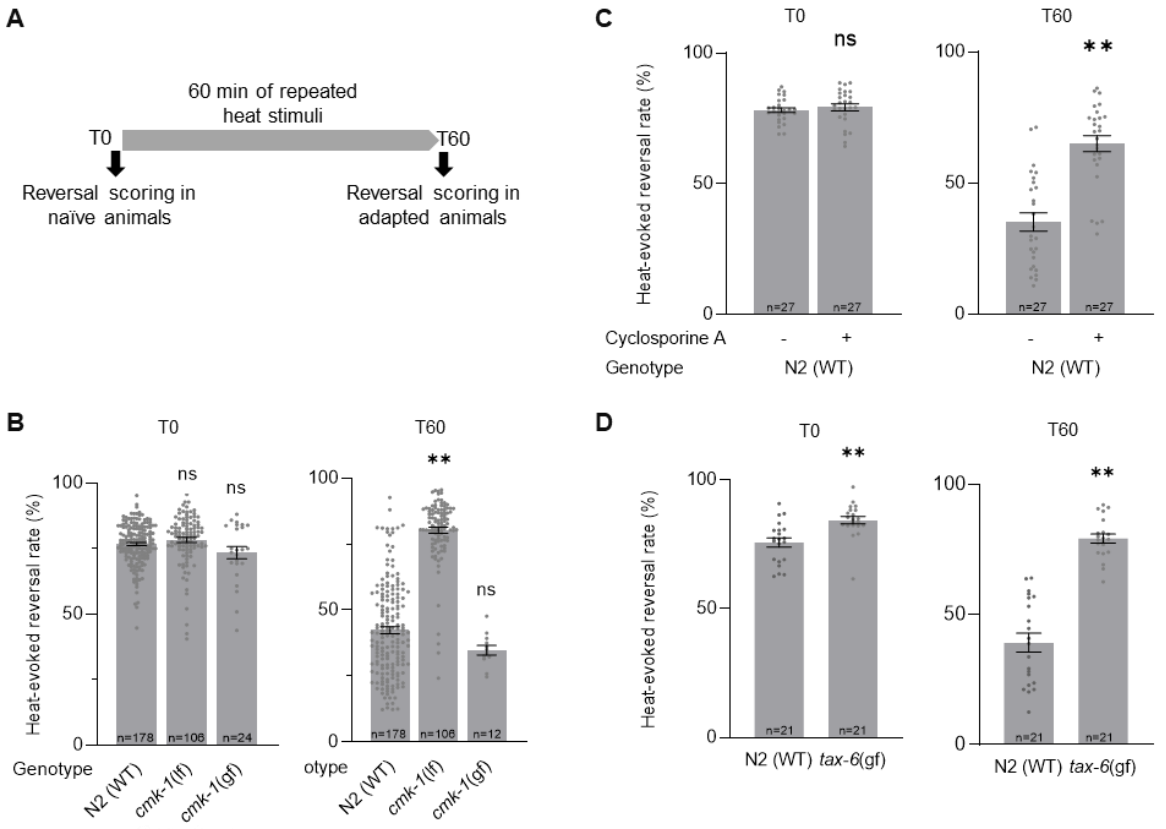

927

928

929 **Figure 2 Impact of loss and gain of CMK-1 and TAX-6/CnA function on *C. elegans* thermo-**
930 **nociceptive response**

931 **A**. Schematic of the scoring procedure. Heat-evoked reversals were first scored in naïve adult *C.*
932 *elegans* that had never been exposed to thermal stimuli (T0), animals exposed to 4 s heat pulses
933 every 20 s during 60 min, prior to an endpoint scoring after adaptation (T60). **B-D**. Heat-evoked
934 reversal scored in the indicated genotypes. Results as fraction of reversing animals. Each point
935 corresponds to one assay scoring at least 50 animals. Average (grey bars) and s.e.m (error bars)
936 with indicated *n* representing the number of independent assays. *cmk-1(gf)* is *cmk-1(syb1633)*.
937 *cmk-1(lf)* is *cmk-1(ok287)*. *tax-6(gf)* is *tax-(j107)*. For Calcineurin inhibition, 10 µM Cyclosporin A
938 was used 24 prior to experiments. **, $p<.01$ and *, $p<.05$ versus N2(WT) control in the specific
939 condition by Bonferroni-Holm post-hocs tests. ns, not significant.

940

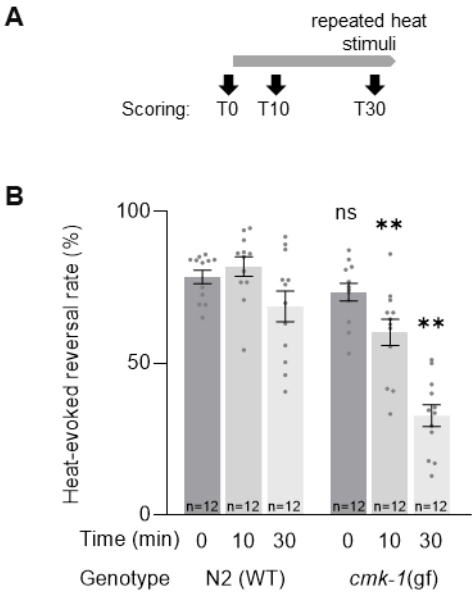

941

942 **Figure 2-supplement 1 CMK-1 overactivating mutation T179D accelerates thermo-**
943 **nociceptive adaptation**

944 **A**. Schematic of the scoring procedure variation, including earlier scoring timepoints after 10
945 and 30 min of repeated noxious heat stimuli. **B**. Heat-evoked reversal scored in the indicated
946 genotypes and reported as in Fig. 2. *cmk-1(gf)* is *cmk-1(syb1633)* harboring the CMK-1(T179D)
947 overactivating mutation. *, p<.01 versus corresponding timepoint in N2(WT) control. ns, not
948 significant.

949

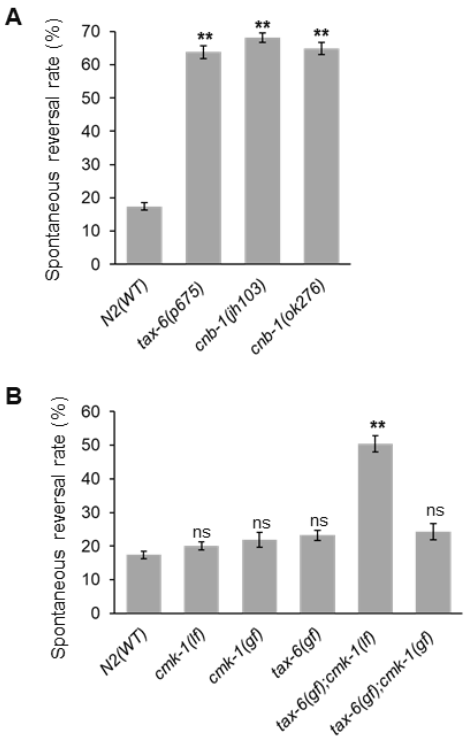

Figure 2-supplement 2 Spontaneous reversal rate in wild type and different single and double mutants

Spontaneous reversal rate scored in the indicated genotypes, in the absence of any noxious heat stimulation. Average (grey bars) and s.e.m (error bars) of $n \geq 12$ assays; each assay scoring at least 50 animals. *, $p<.001$ N2(WT) control. ns, not significant. **A**. Markedly elevated spontaneous reversal rate in *tax-6* and *cnb-1* loss-of-function mutants. **B**. Markedly elevated spontaneous reversal rate in *tax-6(gf);cmk-1(gf)* double mutant, but normal phenotype in other genotypes, as indicated.

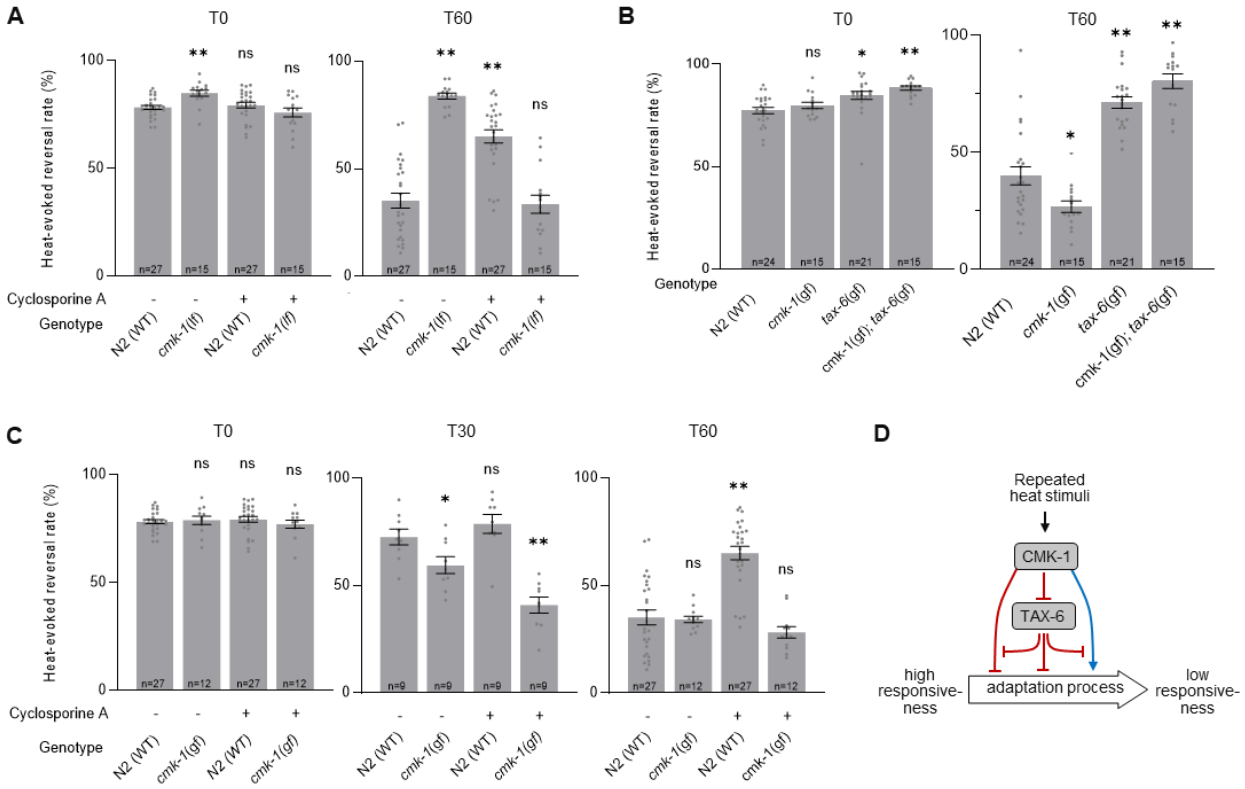

Figure 3 Functional interactions between CMK-1 and TAX-6/CnA in the regulation of thermo-nociceptive adaptation

A-C. Assessment of the impact of joint gain- and loss-of-function manipulations affecting the CMK-1 and TAX-6/CnA pathways. Heat-evoked response in naïve animals (T0) and after 60 min of repeated stimulations (T60), scored and reported as in Fig. 2. **, $p<.01$ and *, $p<.05$ versus N2(WT) control in the specific condition by Bonferroni-Holm post-hocs tests. ns, not significant. **D**. Schematic of a model explaining the multiple antagonistic interactions observed between CMK-1 and TAX-6/CnA signaling. *cmk-1(gf)* is *cmk-1(syb1633)* harboring the CMK-1(T179D) overactivating mutation. *cmk-1(lf)* is *cmk-1(ok287)*. *tax-6(gf)* is *tax-6(jh107)*.

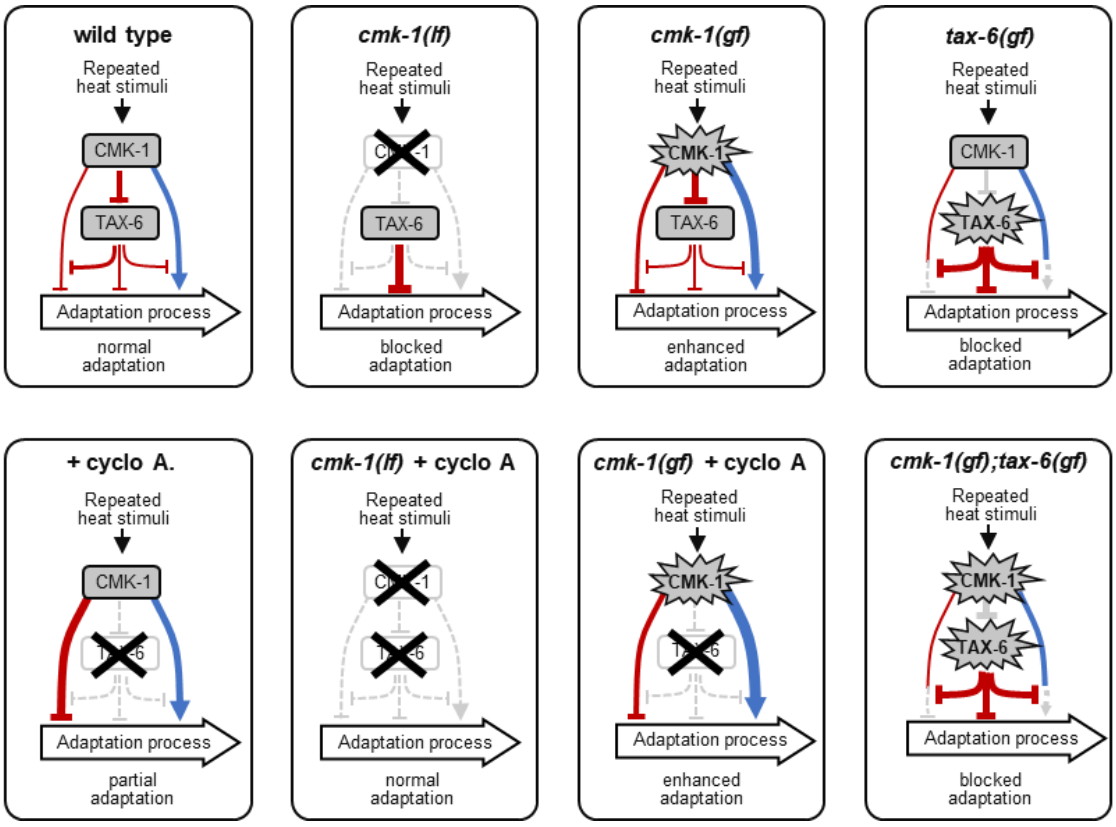

Figure 3- supplement 1 Model of the multiple antagonistic interactions observed between CMK-1 and TAX-6/CnA signaling. Illustration of how the model from Fig. 3D is proposed to be altered for each of the single or combined gain- and loss-of-function manipulations used in Fig. 3. We do not rule out that alternative models might also explain our data, but the model presented in Fig. 3D is the simplest that could explain the complex set of interactions. Blue regular arrows and red flathead arrows indicate positive and negative effects, respectively. Inactivated pathways are drawn with grey dashed lines. The thickness of each line reflects the relative size of an effect. The main assumption of the model is that CMK-1 and TAX-6 are modulators of the adaptation process and the balance between antagonistic effects will determine the level of adaptation. The default adaptation level in the absence of regulation (*cmk-1(lf)* + cyclo A condition) leads to a similar level of adaptation than in wild type. Furthermore, the model considers that the inhibitory effect of TAX-6 on the CMK-1 anti-adaptation branch and the inhibitory effect of TAX-6 on the CMK-1 pro-adaptation branch are not of the same magnitude. Likewise, the two antagonistic direct effects of CMK-1 on adaptation are not of the same magnitude: upon CMK-1 overactivation (*cmk-1(gf)*) the direct pro-adaptation effect of CMK-1 signaling is larger than the anti-adaptation effect. Finally, TAX-6 overactivation has a dominant effect (two panels at the right). cyclo A: Cyclosporin A treatment. *cmk-1(gf)* is *cmk-1(syb1633)* harboring the CMK-1(T179D) overactivating mutation. *cmk-1(lf)* is *cmk-1(ok287)*. *tax-6(gf)* is *tax-6(jh107)*.

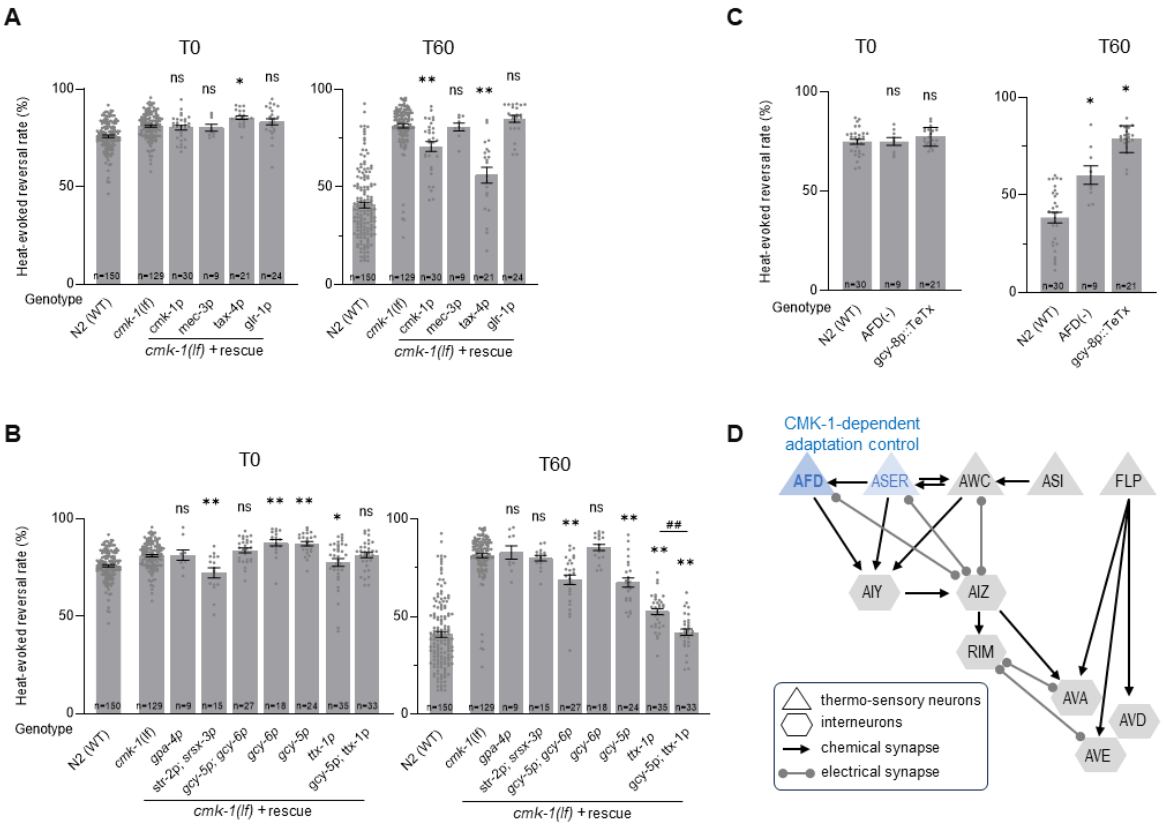

Figure 4. CMK-1 works in AFD and ASER to control thermo-nociceptive adaptation

A-B. Determination of the CMK-1 place of action in the control of thermo-nociceptive adaptation, using cell-specific rescue in *cmk-1(ok287)* (*cmk-1(lf)*) background. Heat-evoked response in naïve animals (T0) and after 60 min of repeated stimulations (T60), scored and reported as in Fig. 2. The promoters used to restore CMK-1 expression are indicated below each bar. **, $p<.01$ and *, $p<.05$ versus *cmk-1(lf)* by Bonferroni-Holm post-hocs tests. ns, not significant. ##, $p<.01$ for the specific contrast between *ttx-1p* and the *gcy-5p;ttx-1p* combination. N2(WT) data are shown for comparison purpose. **C**. Impact of genetic manipulation ablating AFD with a caspase construct (AFD(-)) or inhibiting AFD neurotransmission with TeTx heterologous expression. **, $p<.01$ and *, $p<.05$ versus N2(WT) control by Bonferroni-Holm post-hocs tests **D**. Schematic of the hypothetical circuit controlling noxious-heat evoked reversals, including the *tax-4*-expressing thermo-responsive sensory neurons AFD, AWC, ASER and ASI, the *mec-3*-expressing FLP thermo-nociceptor, and a subset of downstream interneurons known to mediate reversal response, including the *glr-1*-expressing RIM, AVA, AVD, and AVE interneurons. The main loci of action of CMK-1 determined through the cell-specific rescue approach are highlighted in blue.

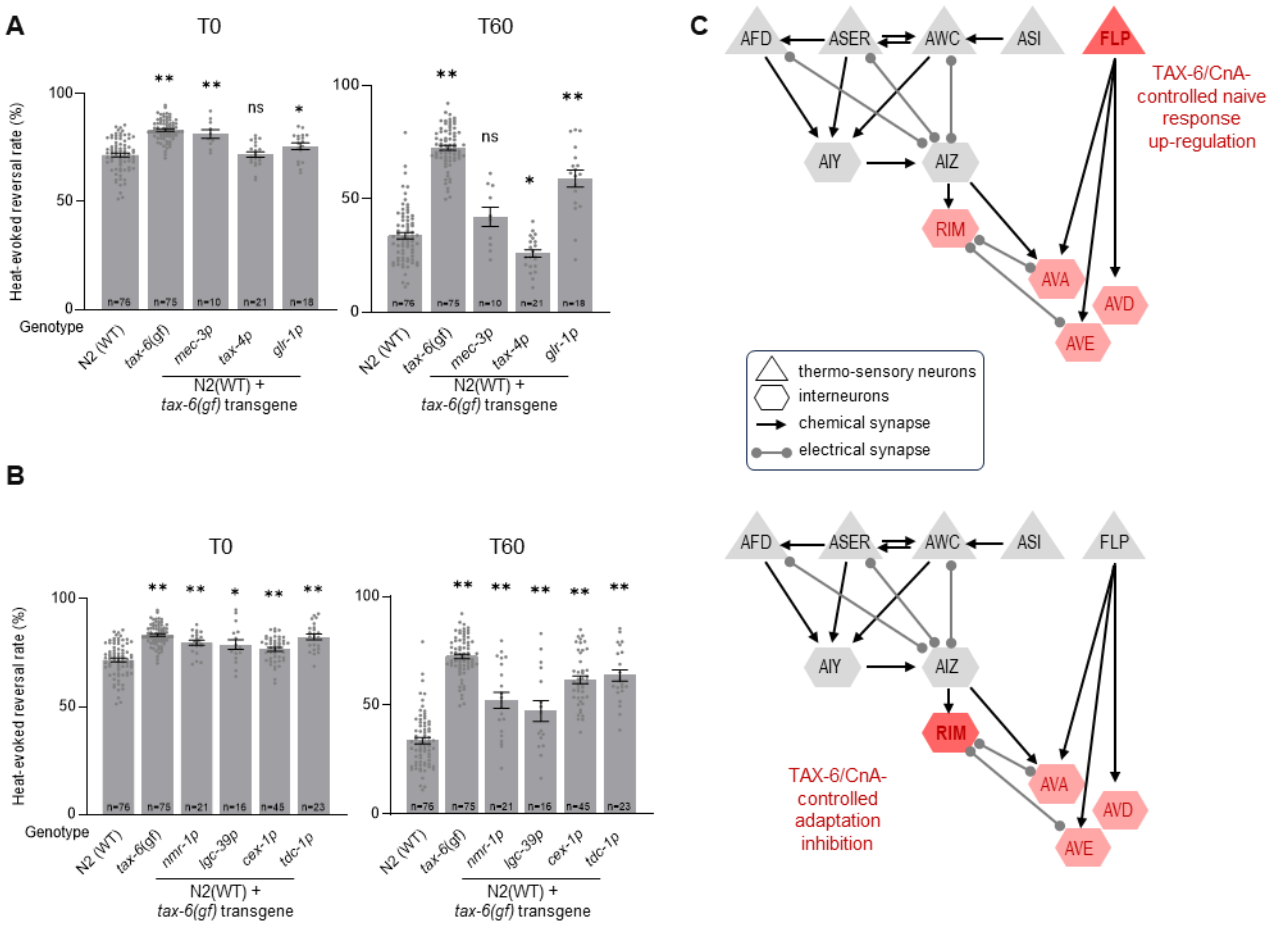

Figure 5. TAX-6/CnA activity in RIM and AVA/AVD/AVE inhibit thermo-nociceptive adaptation

A-B. Determination of the TAX-6/CnA place of action in the control of thermo-nociceptive responses, using cell-specific expression of a TAX-6/CnA gain-of-function mutant. Heat-evoked response in naïve animals (T0) and after 60 min of repeated stimulations (T60), scored and reported as in Fig. 2. The promoters used to drive *tax-6(gf)* cDNA expression are indicated below each bar. **, $p<.01$ and *, $p<.05$ versus N2(WT) by Bonferroni-Holm post-hocs tests. ns, not significant. *tax-6(gf)* mutant data are shown for comparison purpose. **C**. Schematics of the hypothetical circuit controlling noxious-heat evoked reversals as in Fig. 4D, with the main loci of action of TAX-6/CnA highlighted in red. TAX-6/CnA-evoked up-regulation of thermo-nociceptive response in naïve animals (top) and TAX-6/CnA-evoked inhibition of adaptation (bottom).